Chapter 4

Analysis of Dynamic Mathematical Models

> A system is anything that talks to itself. All living systems and organisms ultimately reduce to a bunch of regulators—chemical pathways and neuron circuits—having conversations as dumb as "I want, I want, I want; no, you can't, you can't, you can't."
>
> –*Kevin Kelly*, in *Out of Control*

In the preceding chapters we made the implicit assumption that, in the long-term, the concentrations of species in a chemical reaction network will settle to a (unique) steady state profile, regardless of the initial conditions. This is almost always a safe assumption in dealing with closed chemical reaction networks. However, when considering open networks, more interesting behaviours can occur. In this chapter we introduce mathematical techniques that can be used to explore these dynamic behaviours.

4.1 Phase Plane Analysis

In Chapter 2, we represented the dynamic behaviour of reaction networks by plotting the concentrations of the reactant species as functions of time (in analogy to experimental time-courses). An alternative approach to visualization is to plot concentrations against *one another*.

To provide a concrete example of this technique, consider the biochemical network shown in Figure 4.1, which involves two species, S_1 and S_2. To keep the analysis simple, we suppose that all reactions rates follow mass action (or, equivalently, Michaelis-Menten kinetics with all enzymes operating in their first-order regime). The allosteric inhibition of v_1 will be modelled by presuming strong cooperative binding of n molecules of S_2. We can then write

$$v_1 = \frac{k_1}{1 + (s_2/K)^n}, \qquad v_2 = k_2, \qquad v_3 = k_3 s_1, \qquad v_4 = k_4 s_2, \qquad v_5 = k_5 s_1,$$

where $s_1 = [S_1]$ and $s_2 = [S_2]$, so that

$$\begin{aligned} \frac{d}{dt}s_1(t) &= \frac{k_1}{1 + (s_2(t)/K)^n} - k_3 s_1(t) - k_5 s_1(t) \\ \frac{d}{dt}s_2(t) &= k_2 + k_5 s_1(t) - k_4 s_2(t). \end{aligned} \tag{4.1}$$

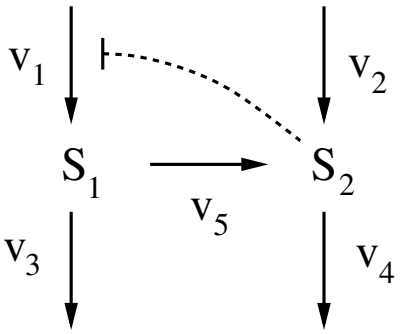

Figure 4.1: Biochemical reaction network. The production of S_1 is allosterically inhibited by S_2. The labels v_i indicate the rates of the corresponding reactions. (They are not mass action rate constants.)

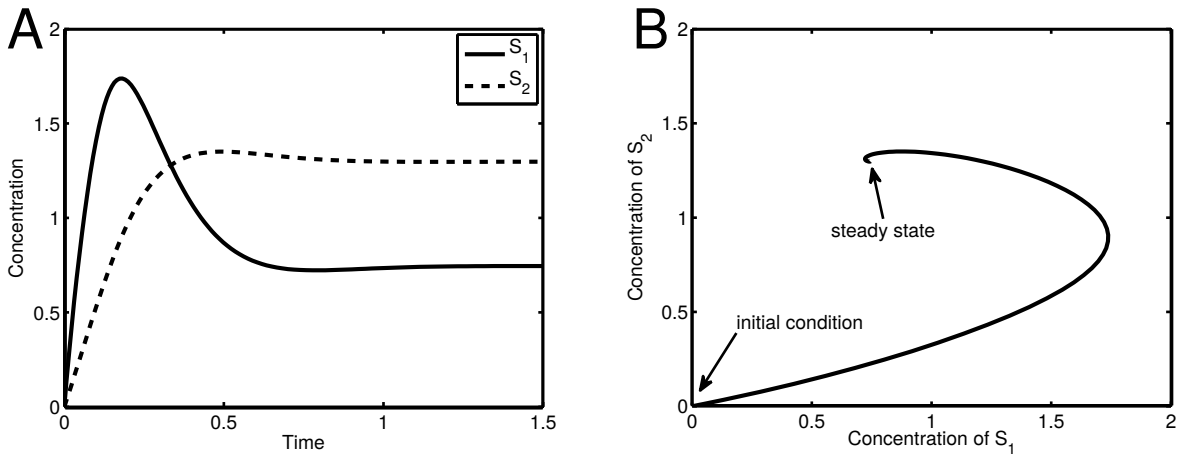

Figure 4.2: Simulation of model (4.1). **A.** Concentrations plotted against time. Both $[S_1]$ and $[S_2]$ overshoot their steady state values before coming to rest. **B.** Concentration $[S_1]$ plotted against concentration $[S_2]$ in the phase plane. Parameter values: (in concentration $\cdot$ time^{-1}) $k_1 = 20$ and $k_2 = 5$; (in concentration) $K = 1$; (in time^{-1}) $k_3 = 5$, $k_4 = 5$, and $k_5 = 2$; and $n = 4$. Units are arbitrary.

Figure 4.2A shows a simulation of the system, starting at initial concentrations of zero. In panel B, the same simulation is displayed by plotting the concentration s_2 against the concentration s_1 in what is called the system's **phase plane** (i.e. the s_1-s_2 plane). The phase plane plot (also called a *phase portrait*) shows the concentrations starting at the initial state $(s_1, s_2) = (0, 0)$ and converging to the steady state. This curve is called a *trajectory.* Comparing with Figure 4.2A, the phase plot emphasizes the time-varying relationship between the two variables, but de-emphasizes the relationship with time itself. Indeed, the direction of motion is not explicitly indicated by the curve, and although each point $(s_1(t), s_2(t))$ corresponds to a particular time instant t, the only time-points that can be easily identified are at $t = 0$ (where the curve starts) and the long-time behaviour ($t \to \infty$, where the curve ends).

The phase portrait allows multiple time-courses (trajectories) to be usefully described in a single plot. This is illustrated in Figure 4.3. Panel A shows the time-course in Figure 4.2A along with a number of other time-courses, each starting from a different initial condition. All of the trajectories reach the same steady state, but the transient behaviour is a meaningless jumble. These same

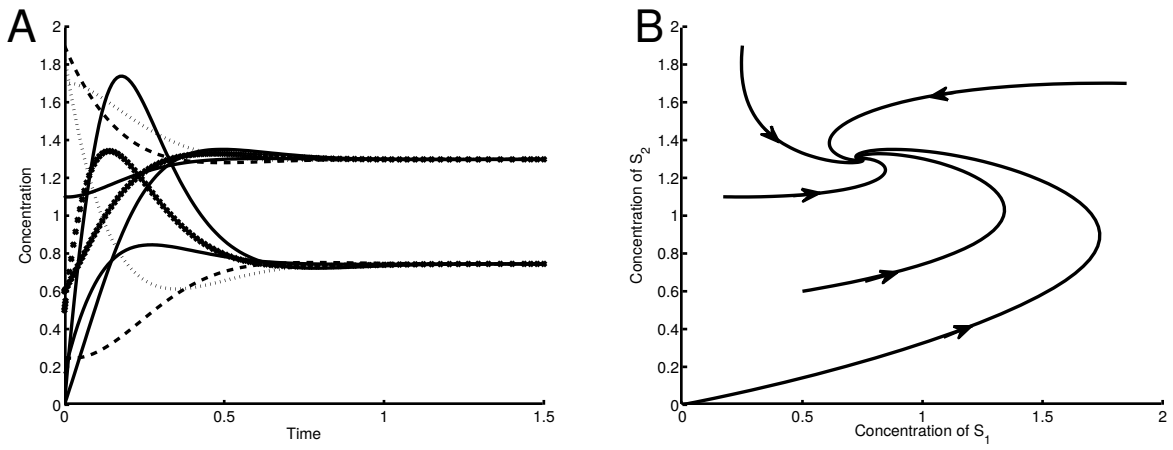

Figure 4.3: Simulations of model (4.1). **A.** Multiple time-courses confirm the steady state concentrations, but the transient behaviour cannot be usefully resolved. **B.** On the phase plane, the individual trajectories provide a unified picture of the dynamic behaviour of the system. Parameters as in Figure 4.2.

simulations are shown as trajectories on a phase plane in Figure 4.3B. Here the overall system behaviour is clear: the trajectories follow a slow spiral as they approach the steady state.

Because phase portraits are two-dimensional, they cannot capture system behaviour when more than two species are involved in the network. However, we will find that insights gained from applying phase-plane analysis to these low-dimensional systems will be directly applicable to larger and more complex models.

4.1.1 Direction fields

A phase portrait can become crowded as more and more trajectories are added. An alternative to drawing all of these curves is to use short arrows to indicate the direction and speed of motion at each point on the phase plane. The resulting plot is called a **direction field**.

Figure 4.4A shows the phase portrait from Figure 4.3B along with the corresponding direction field. The trajectories lie parallel to (i.e. tangent to) the vector field at each point. Additional trajectories can be sketched by simply following the arrows. An analogy can be made to fluid flow, as follows. Imagine a two-dimensional flow (on, for instance, a water table). The vector field describes, at each point, the direction of motion of a particle suspended in the fluid. The trajectories are the paths such particles would traverse as they follow the flow.

A direction field is, in a sense, easier to construct then a phase portrait. To plot trajectories in the phase portrait, simulations of the differential equation model must be carried out. In contrast, the direction field can be determined directly from the differential equation model, as follows. For a general system involving two species concentrations s_1 and s_2:

$$\begin{aligned} \frac{d}{dt}s_1(t) &= f(s_1(t), s_2(t)) \\ \frac{d}{dt}s_2(t) &= g(s_1(t), s_2(t)), \end{aligned}$$

the motion in the phase plane at any given point (s_1, s_2) is given by the vector $(f(s_1, s_2), g(s_1, s_2))$,

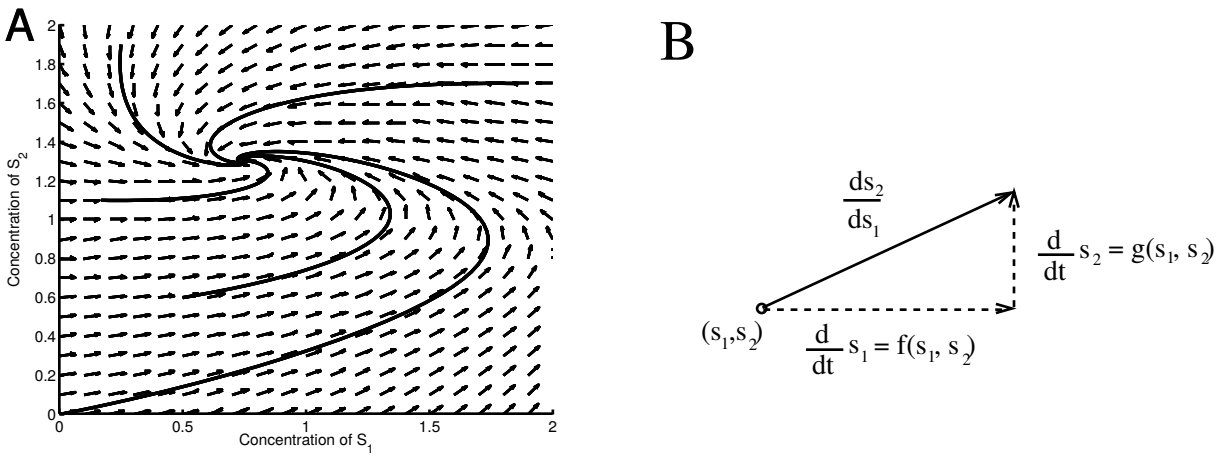

Figure 4.4: Direction field for model (4.1). **A.** The field of arrows indicates the direction of motion at each point. Trajectories are curves that lie tangent to the arrows; they follow the flow. **B.** Arrows in the direction field can be generated directly from the model—no simulation is needed. At each point (s_1, s_2), the direction of the arrow is the slope of s_2 with respect to s_1 ($\frac{ds_2}{ds_1}$). This slope can be determined from the model dynamics, which specify the rates of change of s_2 and s_1. In Panel A, these vectors have been normalized to display a field of arrows of equal length.

as indicated in Figure 4.4B. The direction field can be constructed by selecting a mesh of points (s_1, s_2) in the phase plane and, at each point, drawing an arrow in the appropriate direction.

Exercise 4.1.1 Consider the system

$$\frac{d}{dt}x(t) = -y(t) \qquad\qquad \frac{d}{dt}y(t) = x(t).$$

Sketch the direction field by drawing the direction vectors at the following points in the x-y phase plane: $(1,0)$, $(1,1)$, $(0,1)$, $(-1,1)$, $(-1,0)$, $(-1,-1)$, $(0,-1)$, $(1,-1)$. (Place each vector as an arrow with its tail at the corresponding point in the phase plane.) Can you infer the overall behaviour of the system around its steady state at $(0,0)$? You may want to draw a few more arrows to confirm your conjecture. □

Exercise 4.1.2 Explain why trajectories in the phase portrait cannot cross one another. Hint: consider the direction of motion at the intersection point. □

4.1.2 Nullclines

A key feature of a system's phase portrait are points at which the trajectories 'turn around'—that is, points at which trajectories change their direction with respect to one of the axes. These are the points at which one of the two variables $s_1(t)$ or $s_2(t)$ reaches a local maximum or local minimum.

On the phase plane, these turning points occur whenever a trajectory is directed either vertically (the direction arrow points straight up or down) or horizontally (the arrow points directly left or right). Rather than identify these points by examining the phase portrait, we can determined them directly from the model (because the direction of motion is specified by the model, as in Figure 4.4B). These 'turning points' constitute the system *nullclines*:

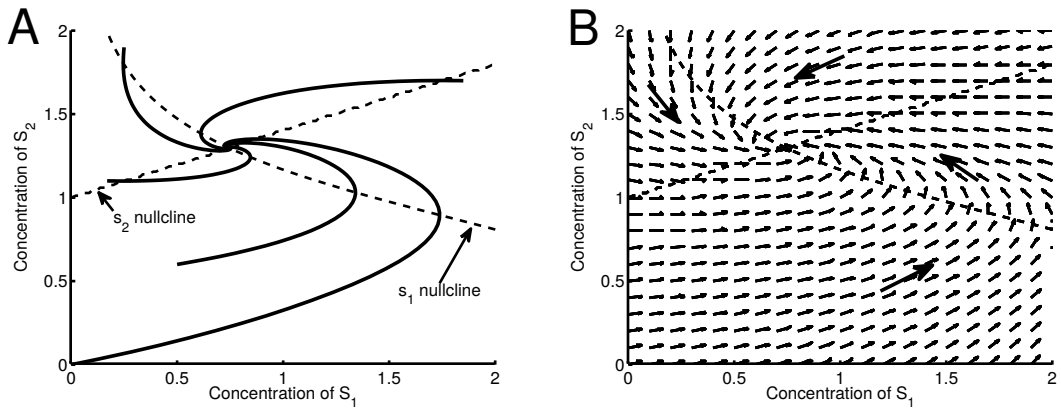

Figure 4.5: Nullclines for model (4.1). **A.** The trajectories intersect the nullclines at turning points. The steady state occurs at the intersection of the nullclines. **B.** The nullclines divide the phase plane into four regions. Since the direction arrows only 'flip' directions at the nullclines, each region is characterized by motion in a particular direction (up/down, left/right), as indicated.

The set of points (s_1, s_2) where $\frac{d}{dt}s_1(t) = f(s_1, s_2) = 0$ is called the s_1**-nullcline**. Likewise, the set of points where $\frac{d}{dt}s_2(t) = g(s_1, s_2) = 0$ is called the s_2**-nullcline**.

Referring to Figure 4.4B, we confirm that points on the s_1-nullcline have direction arrows with no horizontal component (so are oriented vertically), while points on the s_2-nullcline have direction arrows with no vertical component (so are oriented horizontally).

Figure 4.5A shows the phase portrait from Figure 4.3B along with the nullclines. The trajectories cross the s_1 nullcline when they are oriented horizontally and cross the s_2 nullcline when they are oriented vertically. The nullclines intersect at the steady state, since at that point $\frac{ds_1}{dt} = f(s_1, s_2) = 0$ and $\frac{ds_2}{dt} = g(s_1, s_2) = 0$.

The nullclines are shown together with the direction field in Figure 4.5B. The nullclines separate the phase plane into four regions; in each region the direction arrows all have the same up-or-down and left-or-right orientation (since the arrows change these directions only when a nullcline is crossed). Thus, as shown in the figure, a rough picture of system behaviour can be generated by specifying the direction of motion in each of the regions.

The nullclines, like the direction field, can be determined directly from the model—without running simulations. However, the equations $f(s_1, s_2) = 0$ and $g(s_1, s_2) = 0$ are typically nonlinear, and so may not be solvable except via computational software.

Exercise 4.1.3 For model (4.1), the nullclines can be determined analytically. Verify that the s_1-nullcline is given by

$$s_1 = \frac{k_1}{(k_3 + k_5)(1 + (s_2/K)^n)}$$

while the s_2-nullcline is the line

$$s_2 = \frac{k_2 + k_5 s_1}{k_4}.$$

. □

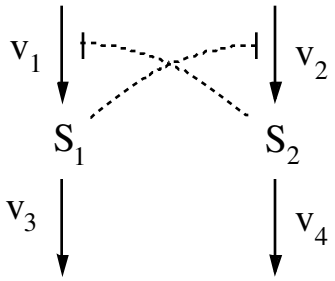

Figure 4.6: Symmetric biochemical network. Each species allosterically inhibits production of the other.

4.2 Stability

The long time (i.e. asymptotic) behaviour of biochemical and genetic networks will be either

- convergence to a steady state; or
- convergence to a sustained periodic oscillation, referred to as **limit cycle** oscillations.

Other dynamic behaviours (divergence and chaos, for example) do not often occur in systems biology models.

For the network studied in the previous section (model (4.1)), we saw that all trajectories converge to a unique steady state. To explore an alternative asymptotic behaviour, we next consider the network in Figure 4.6. This reaction scheme is symmetric—each species allosterically inhibits production of the other, resulting in a mutual antagonism.

With cooperative inhibition and first-order consumption rates, the model is

$$\begin{aligned} \frac{d}{dt}s_1(t) &= \frac{k_1}{1+(s_2(t)/K_2)^{n_1}} - k_3 s_1(t) \\ \frac{d}{dt}s_2(t) &= \frac{k_2}{1+(s_1(t)/K_1)^{n_2}} - k_4 s_2(t). \end{aligned} \tag{4.2}$$

We first consider an asymmetric model parametrization in which $n_1 > n_2$. In this case, the inhibition by S_2 is more effective than the inhibition by S_1. If the other parameters are symmetric ($k_1 = k_2$, $K_1 = K_2$, $k_3 = k_4$) we should expect the model to exhibit a steady state in which the concentration of S_1 is low and the concentration of S_2 is high (the mutual antagonism 'competition' will be won by S_2). This intuition is confirmed by Figure 4.7. Panel A shows two time-courses starting from different initial conditions. Regardless of whether S_1 or S_2 is initially more abundant, the imbalance in inhibition strength leads to the same steady state (low $[S_1]$, high $[S_2]$). The phase portrait in Figure 4.7B confirms this finding. All trajectories converge to the steady state at the intersection of the s_1- and s_2-nullclines, at which S_2 dominates.

Bistability

We next consider the symmetric case. Changing the Hill coefficients so that $n_1 = n_2$, the two species S_1 and S_2 are perfectly balanced. Because neither species has an advantage over the other, we should expect the system to exhibit symmetric behaviour: the two concentrations might converge to the same value (a 'tie game'), or one species will maintain dominance over the other (and emerge

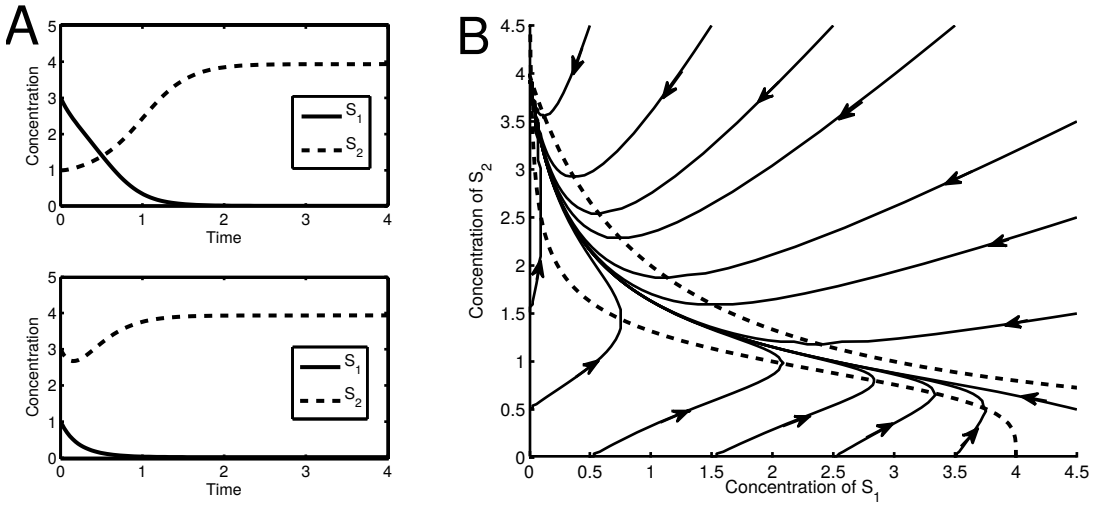

Figure 4.7: Model (4.2) with imbalanced inhibition strength. **A.** Time-series plots show that regardless of the initial condition, the system settles to a steady state with high S_2 concentration and low S_1 concentration. **B.** This phase portrait confirms that all trajectories approach the high-$[S_2]$, low-$[S_1]$ steady state at which the nullclines (dashed lines) intersect. Parameter values: $k_1 = k_2 = 20$ (concentration$\cdot$time^{-1}), $K_1 = K_2 = 1$ (concentration), $k_3 = k_4 = 5$ (time^{-1}), $n_1 = 4$, and $n_2 = 1$. Units are arbitrary.

as the 'winner'). The system's steady-state behaviours are illustrated in Figure 4.8. Panel A shows that the long-time behaviour depends on the initial conditions—whichever species is initially more abundant maintains its dominance. The phase portrait in Panel B shows a symmetric phase plane. Trajectories are attracted to whichever steady state is closer. The region of the phase plane from which trajectories converge to each steady state is called the *basin of attraction* of that steady state. Curves that separate basins of attraction are called *separatrices*. In this perfectly symmetric case, the separatrix is the diagonal.

A system that exhibits two distinct steady states is called **bistable**. (In contrast, a system with a single steady state is called *monostable*.) Bistability provides a system with a type of memory—the system's long-term behaviour reflects its past condition. Biological implications of bistability will be discussed in later chapters.

There are two essential ingredients to bistability: positive feedback and nonlinearity. In the model considered here, the positive feedback is implemented in a double negative feedback loop: each species inhibits production of the other and thus inhibits the inhibition of itself. Thus each species acts to enhances its own production—a positive feedback. (Double negative feedback is sometimes called *derepression*.) Nonlinearity is provided by the cooperative inhibition mechanism.

These two ingredients are necessary for bistability, but they do not guarantee it: the model structure and parameter values must also be properly aligned.

4.2.1 Stable and unstable steady states

The nullclines in Figure 4.8B intersect at the two steady states exhibited by the system, and they also intersect at a third point, on the diagonal. This symmetric point is a steady state for the system, but it will not be observed as a long-time state of the system. The behaviour of the

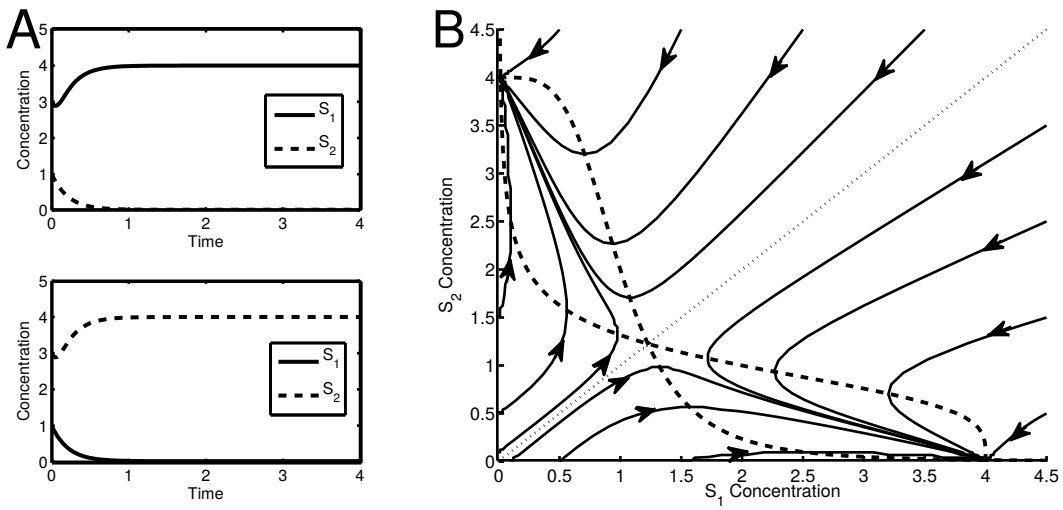

Figure 4.8: Model (4.2) with balanced inhibition strength. **A.** Time-series plots show that the steady state behaviour depends on the initial conditions. Either species can dominate over the other if its initial concentration is larger. **B.** The phase portrait confirms the presence of two steady states at which the nullclines (dashed lines) intersect. Each trajectory converges to the closer steady state. The two basins of attraction are separated by the diagonal (dotted line). Parameter values: $k_1 = k_2 = 20$ (concentration $\cdot$ time^{-1}), $K_1 = K_2 = 1$ (concentration), $k_3 = k_4 = 5$ (time^{-1}), $n_1 = n_2 = 4$. Units are arbitrary.

trajectories near this symmetric steady state is shown more clearly in Figure 4.9. Trajectories near this state are repelled from it; they tend toward one of the other two steady states. We say that this steady state is **unstable** because nearby trajectories diverge away from it. In contrast, the other two steady states in Figure 4.8B—which attract nearby trajectories—are called **stable**. This system thus has two stable steady states and one unstable steady state. The existence of an intermediate unstable steady state is a defining feature of bistable systems.

In theory, the unstable steady state can be maintained by perfectly balanced initial conditions (trajectories balanced on the diagonal will converge to this point). However, any deviation from this balance causes the trajectory to tend toward a stable steady state. This behaviour is illustrated by a standard metaphor for stability: a ball rolling on an undulating slope (Figure 4.10), in which valley bottoms correspond to stable steady states while hilltops correspond to unstable steady states. A ball within a valley is attracted to the valley bottom, and settles to rest. A ball balanced on a hilltop will theoretically remain in that position, but the slightest nudge in any direction will send it rolling toward a valley bottom.

By extending this analogy to three dimensions (Figure 4.11) we can illustrate the stability behaviors of the phase plots in Figures 4.7B and 4.8B. The single valley in Figure 4.11A corresponds to a monostable system. In Panel B, the unstable point attracts trajectories that are perfectly balanced on the ridge, but any imbalance causes trajectories to fall to one of the valley bottoms. Because of the shape of the surface, this unstable point is called a *saddle*. The valleys are the two basins of attraction; the ridge is the separatrix between them.

Exercise 4.2.1 Consider the simple reaction chain $\stackrel{v_1}{\rightarrow} S \stackrel{v_2}{\rightarrow}$. Let $s = [S]$. If $v_1 = k_1$ (constant) and $v_2 = k_2 s$, then there is no feedback, and the system will be monostable, with steady state $s = k_1/k_2$.

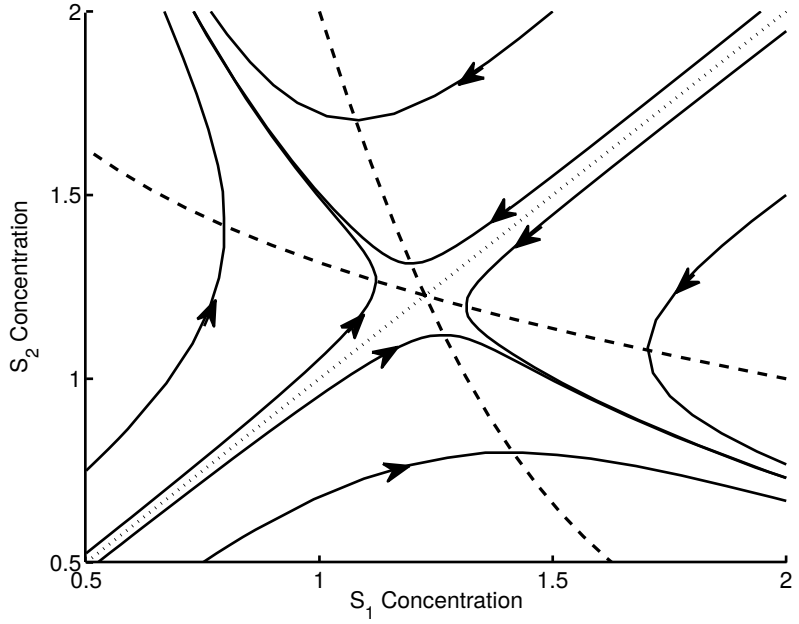

Figure 4.9: Model (4.2) with balanced inhibition strength: unstable steady state. Figure 4.8B shows the nullclines intersecting three times. This close-up of the middle intersection shows that trajectories are repelled from this unstable steady state. The dashed lines are the nullclines. The dotted line (on the diagonal) is the separatrix that forms the boundary between the two basins of attraction.

a) Alternatively, if $v_1 = k_1 s$, then S enhances its own production in a positive feedback. Take the consumption rate to be nonlinear: $v_2 = k_2 s^2$. Verify that in this case the system exhibits two steady states: one with $s = 0$ and one with $s = k_1/k_2$. In this one-dimensional case, the stability of these steady states can be determined by evaluating the rate of change of s near each point. For instance, when s is near zero, $s^2 \ll s$, so $k_1 s^2$ will be small compared to $k_2 s$. The rate of change $\frac{d}{dt}s(t)$ will then be positive, so $s(t)$ increases away from the steady state at $s = 0$; this steady state is unstable. Verify that the steady state $s = k_1/k_2$ is stable by determining the sign of $\frac{d}{dt}s(t)$ above and below k_1/k_2.

b) Consider the case $v_1 = k_0 + \frac{k_1 s^2}{k_2 + s^2}$ and $v_2 = k_3 s$, in which the system exhibits positive feedback and significant nonlinearity. In this case, the system is bistable for appropriate values of the parameters. Take $k_0 = 6/11$, $k_1 = 60/11$, $k_2 = 11$ and $k_3 = 1$ and verify that $s = 1$, $s = 2$ and $s = 3$ are all steady states. Evaluate the rate of change $\frac{d}{dt}s(t)$ around these points to verify that $s = 1$ and $s = 3$ are stable, while $s = 2$ is unstable.

□

So far, we have determined stability from system phase portraits. We next introduce a technique for stability analysis that does not rely on graphical representations and is not restricted to two-species networks.

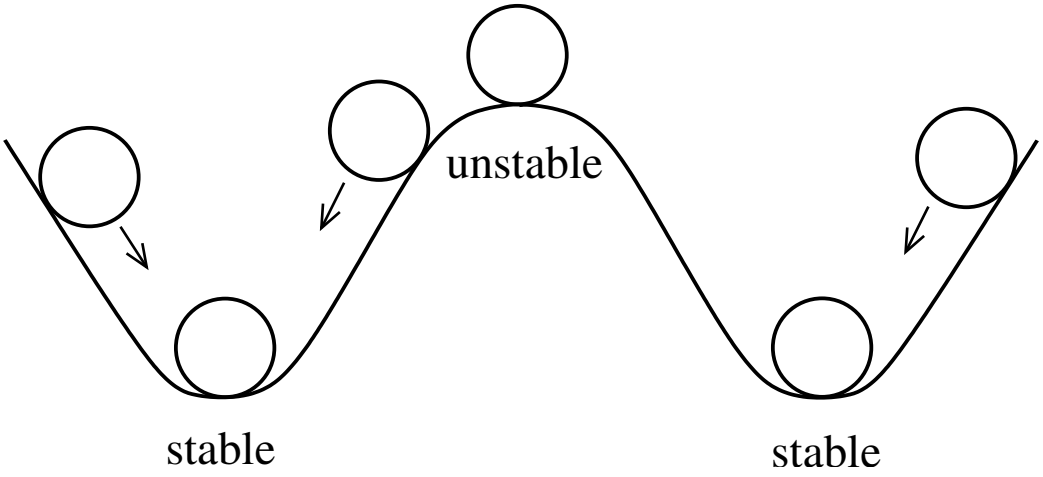

Figure 4.10: Stability and instability. In this analogy of a ball rolling on an undulating slope, the valley bottoms correspond to stable steady states; balls in each valley are attracted to the valley bottom, where they settle to rest. The hilltops correspond to unstable states; a ball perfectly balanced on a hilltop will stay there, but any deviation will topple the ball toward one of the valley bottoms. The slope shown here corresponds to a bistable system, with an unstable steady state separating the basins of attractions (the valleys) of the two stable steady states.

4.2.2 Linearized stability analysis

The behaviour of trajectories near a steady state is called *local* behaviour. As we shall see in this section, the local behaviour of any nonlinear system can be approximated by a linear system. This approximation, called the *linearization*, can be used to test for stability of steady states.

Linearization

As reviewed in Appendix B, we can approximate any function $f(s)$ near a particular point $s = \bar{s}$ by the tangent line centered at $\bar{s}$, as illustrated in Figure 4.12:

$$f(s) \approx f(\bar{s}) + \frac{df}{ds}(\bar{s}) \cdot (s - \bar{s}).$$

The tangent line is called the *linearization* (or *linear approximation*) of $f(s)$ at $s = \bar{s}$.

Exercise 4.2.2 Consider the Michaelis-Menten rate law

$$f(s) = \frac{V_{\max} s}{K_M + s}$$

a) Determine the linear approximation of $f(s)$ at an arbitrary point $\bar{s}$.
b) Verify that the linear approximation centered at $\bar{s} = 0$ has the form of a (first-order) mass action rate law.
c) Verify that when $\bar{s}$ is large compared to K_M (so that $K_M + \bar{s} \approx \bar{s}$), the linearization is almost horizontal (i.e. it approximates a zeroth-order rate law). □

Figure 4.11: Monostability and bistability. **A.** For a monostable system, there is a single valley bottom, representing a unique steady state to which all trajectories converge. **B.** A bistable system corresponds to a pair of valleys, separated by a ridge. The low point of the ridge is the unstable steady state (a saddle point). Most trajectories settle to one of the valley bottoms, but trajectories that remain perfectly balanced on the ridge will settle to the unstable saddle point.

Linear approximations can also be constructed for functions of more than one variable. For a function of two variables, $f(s_1, s_2)$, the linearization centered at a point $(s_1, s_2) = (\bar{s}_1, \bar{s}_2)$ is

$$f(s_1, s_2) \approx f(\bar{s}_1, \bar{s}_2) + \frac{\partial f}{\partial s_1}(\bar{s}_1, \bar{s}_2)\cdot(s_1 - \bar{s}_1) + \frac{\partial f}{\partial s_2}(\bar{s}_1, \bar{s}_2)\cdot(s_2 - \bar{s}_2). \tag{4.3}$$

(Readers unfamiliar with partial derivatives may wish to consult appendix B.) This approximation is valid for arguments (s_1, s_2) near the point $(\bar{s}_1, \bar{s}_2)$. This linearization corresponds to a tangent plane approximating the surface $z = f(s_1, s_2)$, as in Figure 4.13.

Exercise 4.2.3 Consider the rate law for a competitively inhibited enzyme:

$$f(s, i) = \frac{V_{\max} s}{K_M(1 + i/K_i) + s}$$

Determine the linear approximation centered at $(s, i) = (1, 0)$. □

Now, consider the general two-species system introduced in Section 4.1.1:

$$\begin{aligned} \frac{d}{dt}s_1(t) &= f(s_1(t), s_2(t)) \\ \frac{d}{dt}s_2(t) &= g(s_1(t), s_2(t)). \end{aligned}$$

We will construct linear approximations to $f(s_1, s_2)$ and $g(s_1, s_2)$. By centering these linearizations at a steady state $(\bar{s}_1, \bar{s}_2)$ we have (because $f(\bar{s}_1, \bar{s}_2) = 0$ and $g(\bar{s}_1, \bar{s}_2) = 0$),

$$\begin{aligned} \frac{d}{dt}s_1(t) &= f(s_1(t), s_2(t)) \approx \frac{\partial f}{\partial s_1}(\bar{s}_1, \bar{s}_2)\cdot(s_1(t) - \bar{s}_1) + \frac{\partial f}{\partial s_2}(\bar{s}_1, \bar{s}_2)\cdot(s_2(t) - \bar{s}_2) \\ \frac{d}{dt}s_2(t) &= g(s_1(t), s_2(t)) \approx \frac{\partial g}{\partial s_1}(\bar{s}_1, \bar{s}_2)\cdot(s_1(t) - \bar{s}_1) + \frac{\partial g}{\partial s_2}(\bar{s}_1, \bar{s}_2)\cdot(s_2(t) - \bar{s}_2). \end{aligned} \tag{4.4}$$

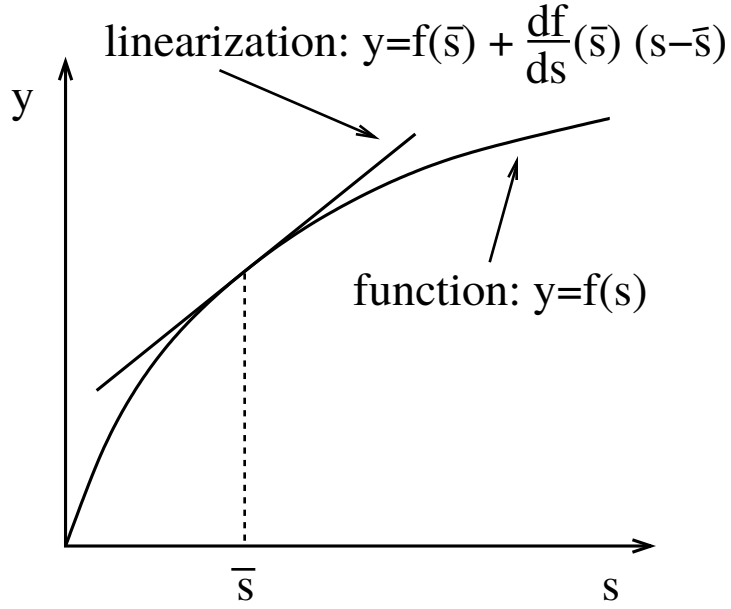

Figure 4.12: Linear approximation of a function of a single variable. The tangent line centered at $s = \bar{s}$ provides a good approximation to the function $f(s)$ when the argument s is near $\bar{s}$.

Because we will be applying this linearization to address stability, we are particularly interested in the behaviour of trajectories whose initial conditions are near a steady state. If the steady state is stable, these trajectories will converge to the steady state; if it is unstable, they will diverge. We can think of these trajectories as small displacements from the steady state that either shrink or grow with time. To focus on these displacements, we introduce a change of variables that describes these deviations explicitly:

$$x_1(t) = s_1(t) - \bar{s}_1 \qquad\qquad x_2(t) = s_2(t) - \bar{s}_2.$$

A small displacement from the steady state $(\bar{s}_1, \bar{s}_2)$ thus corresponds to a value of (x_1, x_2) near $(0, 0)$. The dynamics of these displacement variables is easily described. Observing that

$$\frac{d}{dt}x_1(t) = \frac{d}{dt}s_1(t) + 0 \qquad \text{and} \qquad \frac{d}{dt}x_2(t) = \frac{d}{dt}s_2(t) + 0,$$

we have the approximate dynamics (from equation (4.4)):

$$\begin{aligned} \frac{d}{dt}x_1(t) &= \frac{\partial f}{\partial s_1}(\bar{s}_1, \bar{s}_2)\, x_1(t) + \frac{\partial f}{\partial s_2}(\bar{s}_1, \bar{s}_2) x_2(t) \\ \frac{d}{dt}\, x_2(t) &= \frac{\partial g}{\partial s_1}(\bar{s}_1, \bar{s}_2)\, x_1(t) + \frac{\partial g}{\partial s_2}(\bar{s}_1, \bar{s}_2)\, x_2(t), \end{aligned}$$

which is valid for (x_1, x_2) near $(0, 0)$. This set of differential equations forms a **linear system**. The steady state $(x_1, x_2) = (0, 0)$ of this linear system corresponds to the steady state $(\bar{s}_1, \bar{s}_2)$ of the original nonlinear system. We next present a procedure for testing stability for this linear system; this will determine stability for the nonlinear system as well.

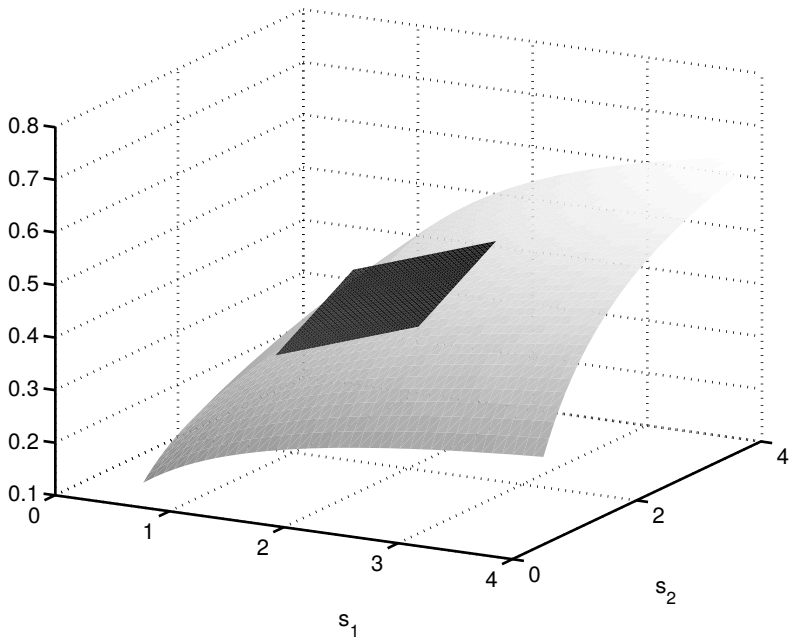

Figure 4.13: Linear approximation of a function of two variables. The tangent plane centered at $(s_1, s_2) = (\bar{s}_1, \bar{s}_2)$ provides a good approximation to the function $f(s_1, s_2)$ when the argument (s_1, s_2) is near $(\bar{s}_1, \bar{s}_2)$.

Stability analysis for linear systems

The general form for a two-state linear system is

$$\begin{aligned} \frac{d}{dt}x_1(t) &= ax_1(t) + bx_2(t) \\ \frac{d}{dt}x_2(t) &= cx_1(t) + dx_2(t). \end{aligned} \tag{4.5}$$

This system can be solved explicitly. Solutions take the form

$$\begin{aligned} x_1(t) &= c_{11}e^{\lambda_1 t} + c_{12}e^{\lambda_2 t} \\ x_2(t) &= c_{21}e^{\lambda_1 t} + c_{22}e^{\lambda_2 t}. \end{aligned} \tag{4.6}$$

The constants c_{ij} depend on the initial conditions, but the values of λ_1 and λ_2 are inherent to the system. They are the *eigenvalues* of the system's **Jacobian**, which is constructed from system (4.5) as the matrix

$$\mathbf{J} = \begin{bmatrix} a & b \\ c & d \end{bmatrix}.$$

The eigenvalues of this matrix are the roots of the quadratic equation

$$\lambda^2 - (a+d)\lambda + (ad - bc) = 0.$$

Applying the quadratic formula gives

$$\lambda_1 = \frac{(a+d) + \sqrt{(a+d)^2 - 4(ad-bc)}}{2}, \qquad \lambda_2 = \frac{(a+d) - \sqrt{(a+d)^2 - 4(ad-bc)}}{2}. \tag{4.7}$$

Depending on the sign of the discriminant $(a+d)^2 - 4(ad-bc)$, these eigenvalues may be real-valued or complex-valued.*

Exercise 4.2.4 Verify that if either of the off-diagonal terms b or c is zero, then the eigenvalues of the Jacobian are the diagonal entries of the matrix: $\lambda_1 = a$ and $\lambda_2 = d$. □

Exercise 4.2.5 Consider the system

$$\begin{aligned} \frac{d}{dt}x_1(t) &= -\frac{5}{3}x_1(t) + \frac{1}{3}x_2(t) \\ \frac{d}{dt}x_2(t) &= \frac{2}{3}x_1(t) - \frac{4}{3}x_2(t) \end{aligned} \tag{4.8}$$

Find the eigenvalues of the Jacobian matrix

$$\begin{bmatrix} -5/3 & 1/3 \\ 2/3 & -4/3 \end{bmatrix}.$$

Use the formula (4.6) to determine the solution of system (4.8) that satisfies initial conditions $x_1(0) = \frac{1}{3}$, $x_2(0) = \frac{5}{3}$. Hint: the initial conditions provide two constraints on the unknowns c_{ij}. Two more constraints can be determined by evaluating the time-derivative of the solutions (4.6) at $t = 0$ and substituting those derivatives and the initial conditions into system (4.8). □

The general behaviour of the solutions (4.6) depends on the nature of the exponential functions $e^{\lambda_1 t}$ and $e^{\lambda_2 t}$. To classify the behaviour of these functions, we consider two cases.

Case I. The discriminant is non-negative, so that λ_1 and λ_2 are real numbers. We note that

i) If both eigenvalues are negative (e.g. $\lambda_1 = -3$, $\lambda_2 = -1$), then both solutions $x_1(t)$ and $x_2(t)$ tend to zero (regardless of the values of the constants c_{ij}). Because (x_1, x_2) is the displacement of (s_1, s_2) from $(\bar{s}_1, \bar{s}_2)$, the steady state $(\bar{s}_1, \bar{s}_2)$ is stable. In this case, the steady state is called a *stable node*.

ii) if *either* eigenvalue is positive (e.g. $\lambda_1 = -3$, $\lambda_2 = 1$), then most solutions diverge (because one of the exponentials grows indefinitely). Thus the displacement of $(s_1,\ s_2)$ from $(\bar{s}_1, \bar{s}_2)$ grows; the steady state is unstable. If both eigenvalues are positive, then all trajectories diverge, and the steady state is called an *unstable node*. If one eigenvalue is negative and the other is positive, then the steady state is called a *saddle point*. (The unstable steady state in Figure 4.8 is a saddle point. The negative eigenvalue causes perfectly balanced trajectories to approach the saddle point along the diagonal, as in Figure 4.11B.)

*Complex numbers, e.g. $3+4i$, involve the square root of -1, denoted i. The generic complex number $x+yi$ has x as its *real part* and y as its *imaginary part*. For the complex number $3+4i$, the real part is 3 and the imaginary part is 4 (not $4i$).

Case II. The discriminant $(a+d)^2 - 4(ad-bc)$ is negative, so the eigenvalues are complex-valued. In this case, referring back to equation (4.7), let

$$\alpha = \frac{a+d}{2} \qquad \text{and} \qquad \beta = \frac{\sqrt{-((a+d)^2 - 4(ad-bc))}}{2}.$$

We can then write the eigenvalues as*

$$\lambda_1 = \alpha + \beta i \qquad \text{and} \qquad \lambda_2 = \alpha - \beta i$$

Because the solutions (4.6) involve the terms $e^{\lambda_1 t}$ and $e^{\lambda_2 t}$, we will need to evaluate the exponential of complex numbers. *Euler's formula* states that

$$\begin{aligned} e^{\lambda_1 t} = e^{(\alpha+\beta i)t} &= e^{\alpha t}(\cos(\beta t) + i\sin(\beta t)) \\ e^{\lambda_2 t} = e^{(\alpha-\beta i)t} &= e^{\alpha t}(\cos(-\beta t) + i\sin(-\beta t)) = e^{\alpha t}(\cos(\beta t) - i\sin(\beta t)) \end{aligned}$$

Substituting these expressions into the solution formulas (4.6), we find

$$\begin{aligned} x_1(t) &= c_{11}e^{\alpha t}(\cos(\beta t) + i\sin(\beta t)) + c_{12}e^{\alpha t}(\cos(\beta t) - i\sin(\beta t)) \\ x_2(t) &= c_{21}e^{\alpha t}(\cos(\beta t) + i\sin(\beta t)) + c_{22}e^{\alpha t}(\cos(\beta t) - i\sin(\beta t)). \end{aligned} \tag{4.9}$$

These expressions may raise some eyebrows. If $x_1(t)$ and $x_2(t)$ describe the displacement of species concentrations from their steady state values, how can they possibly take complex values? This issue is resolved by a special property of these formulas: if the initial displacements $x_1(0)$ and $x_2(0)$ are specified as real numbers, then the corresponding constants c_{ij} guarantee that the formulas in (4.9) evaluate to real numbers. (The imaginary parts of these expressions will cancel to zero. See Problem 4.8.2 for an example.)

Having resolved the unsettling appearance of the solution formulas (4.9), we next consider their behaviour. In each formula the exponential $e^{\alpha t}$ is multiplied by terms involving cosines and sines. These sines and cosines contribute an oscillatory component to the trajectories, but they have no influence over whether the solutions divergence or convergence. The long term behaviour is determined solely by the exponential term $e^{\alpha t}$. We note that:

i) If α, the real part of the eigenvalues, is negative, then the solutions converge to zero. In this case the steady state is stable. It is called a *stable spiral point*, or *focus*. Solutions will exhibit damped oscillations as they converge.

ii) If α, the real part of the eigenvalues, is positive, then the solutions diverge. The steady state is unstable, and is called an *unstable spiral point*.

Fortunately, the conclusions about stability in the real-valued case and the complex-valued case are consistent. Because the real part of a real number is simply the number itself, we arrive at the following general statement.

Linearized Stability Criterion

i) If both eigenvalues of the Jacobian have negative real part then the steady state is *stable*.

ii) if *either* eigenvalue has positive real part, then the steady state is *unstable*.

*For a negative number y, we have $\sqrt{y} = (\sqrt{-y})(\sqrt{-1}) = (\sqrt{-y})i$.

We have not addressed the case of eigenvalues with zero real part. This occurs only for systems that exhibit certain symmetries, and is rarely encountered in models of biochemical and genetic networks. (When both eigenvalues have zero real part the trajectories are periodic; they follow circular arcs around the steady state, which is then called a *center*.)

We derived the linearized stability criterion for systems involving two species. It can be shown that this eigenvalue-based criterion applies to systems of any size. (In particular, a steady state s^{ss} of a one-dimensional system $\frac{d}{dt}x(t) = f(x(t))$ is stable if the Jacobian, which is simply $\frac{d}{dx}f(x)$, is negative at x^{ss}. This Jacobian is a single number, which is also the eigenvalue.)

In summary, to apply the linearized stability criterion to a nonlinear model:

1. Identify a steady state of interest.
2. Construct the system Jacobian at that point (by taking the appropriate partial derivatives).
3. Evaluate the eigenvalues of the Jacobian.
4. Check the sign of their real parts.

To illustrate, consider model (4.2), with symmetric parameter values as in Figure 4.8, except $n_1 = n_2 = 2$:

$$\frac{d}{dt}s_1(t) = \frac{20}{1+s_2^2(t)} - 5s_1(t) \qquad\qquad \frac{d}{dt}s_2(t) = \frac{20}{1+s_1^2(t)} - 5s_2(t).$$

Defining $f(s_1, s_2) = \frac{20}{1+s_2^2} - 5s_1$ and $g(s_1, s_2) = \frac{20}{1+s_1^2} - 5s_2$, we construct the system Jacobian as

$$\mathbf{J}(s_1, s_2) = \begin{bmatrix} \frac{\partial f}{\partial s_1} & \frac{\partial f}{\partial s_2} \\ \frac{\partial g}{\partial s_1} & \frac{\partial g}{\partial s_2} \end{bmatrix} = \begin{bmatrix} -5 & -\frac{20}{(1+s_2^2)^2}2s_2 \\ -\frac{20}{(1+s_1^2)^2}2s_1 & -5 \end{bmatrix}.$$

To determine the steady state concentration profiles, we must solve the system of equations

$$\frac{20}{1+s_2^2} - 5s_1 = 0 \qquad\qquad \frac{20}{1+s_1^2} - 5s_2 = 0.$$

The three solutions (the system is bistable) can be found numerically as

$$(\bar{s}_1, \bar{s}_2) = (3.73, 0.268), \quad (1.38, 1.38), \quad (0.268, 3.73).$$

Evaluating the Jacobian at each of these three points, and determining the corresponding eigenvalues, we have

$$\mathbf{J}(3.73, 0.268) = \begin{bmatrix} -5 & -9.33 \\ -0.671 & -5 \end{bmatrix}, \lambda_1 = -2.50,\ \lambda_2 = -7.50$$

$$\mathbf{J}(1.38, 1.38) = \begin{bmatrix} -5 & -6.54 \\ -6.54 & -5 \end{bmatrix}, \lambda_1 = -11.5,\ \lambda_2 = 1.55$$

$$\mathbf{J}(0.268, 3.73) = \begin{bmatrix} -5 & -0.671 \\ -9.33 & -5 \end{bmatrix}, \lambda_1 = -7.50,\ \lambda_2 = -2.50$$

We thus confirm that the balanced steady state (1.38,1.38) is a saddle point, while the other two steady states are stable nodes.

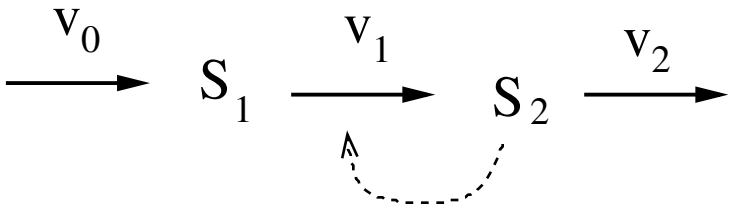

Figure 4.14: Autocatalytic biochemical reaction network.

Exercise 4.2.6 Perform a linearized stability analysis for the model (4.2) with unbalanced inhibition as specified by the parameter values in Figure 4.7. The steady state is $(\bar{s}_1, \bar{s}_2) = (0.0166, 3.94)$. □

Exercise 4.2.7 Solve for the steady state of the system

$$\begin{aligned} \frac{d}{dt}s_1(t) &= V_0 - k_1 s_1(t) \\ \frac{d}{dt}s_2(t) &= k_1 s_1(t) - \frac{V_2 s_2(t)}{K_M + s_2(t)}. \end{aligned}$$

Assume that $V_2 > V_0$. Use linearized stability analysis to verify that this steady state is stable for all (non-negative) values of the model parameters. □

4.3 Limit Cycle Oscillations

So far, our analysis of long-term behaviour has been restricted to steady states. We next consider systems whose long term behaviour is sustained oscillation.

We make a distinction between *damped* oscillations, which display ever-decreasing amplitude and converge eventually to a steady-state, and *persistent* (or *sustained*) oscillations, which are periodic and continue indefinitely. These two behaviours look very different in the phase plane, but they can look similar in time series unless simulations are run for sufficiently long time periods.

As an example of a system that displays persistent oscillatory behaviour, we consider the network in Figure 4.14. In this scheme species S_2 allosterically activates its own production. This sort of positive feedback, called *autocatalysis*, is common in biology.

We model the network as

$$\begin{aligned} \frac{d}{dt}s_1(t) &= k_0 - k_1[1 + (s_2(t)/K)^n]s_1(t) \\ \frac{d}{dt}s_2(t) &= k_1[1 + (s_2(t)/K)^n]s_1(t) - k_2 s_2, \end{aligned} \tag{4.10}$$

The allosteric activation is presumed to be strongly cooperative.

Intuition suggests that this system might be prone to oscillations: the positive feedback will cause a continual increase in the rate of S_2 production until the pool of S_1 is depleted. The S_2 concentration will then crash, and stay low until more S_1 is available, at which point the cycle can repeat.

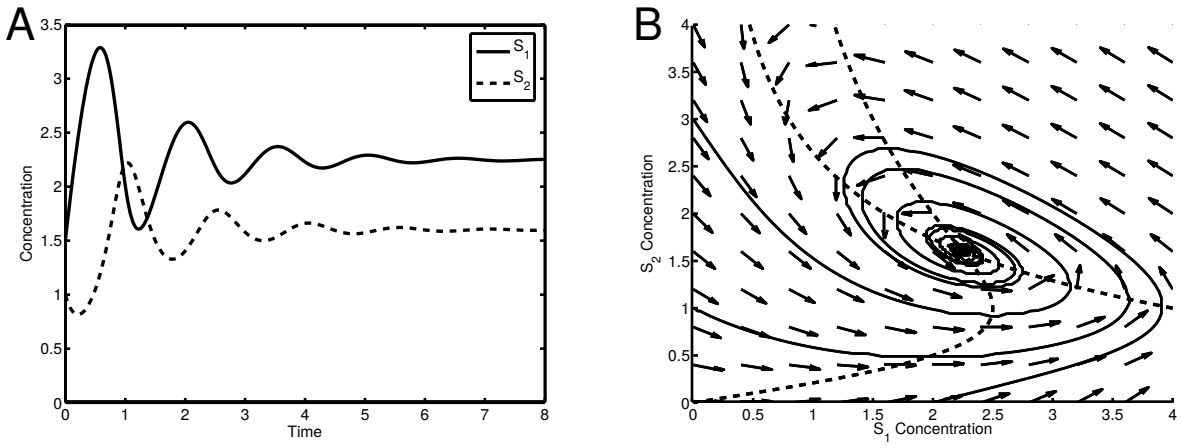

Figure 4.15: Model (4.10) with moderate nonlinearity. **A.** Time series. The species concentrations exhibit damped oscillations as they converge to steady state. **B.** Phase plane. Damped oscillations correspond to trajectories (solid curves) spiraling toward the steady state at the intersection of the nullclines (dashed curves). Parameter values: $k_0 = 8$ (concentration $\cdot$ time^{-1}), $k_1 = 1$ (time^{-1}), $K = 1$ (concentration), $k_2 = 5$ (time^{-1}) and $n = 2$. Units are arbitrary.

Figure 4.15 shows the system's behaviour when the Hill coefficient has value $n = 2$. The model exhibits a single steady state—a stable spiral point. Damped oscillations of the species concentrations are evident in both the times series (Panel A) and the phase portrait (Panel B). These damped oscillations suggest that the system may be "close" to displaying persistent periodic behaviour.

Next, consider the behaviour when the Hill coefficient is raised to $n = 2.5$, shown in Figure 4.16. In the times series (Panel A), we see a short transient followed by sustained periodic behaviour. The phase portrait (Panel B) shows a cyclic track, called a **limit cycle**, to which all trajectories are attracted. Comparing with the phase portrait in Figure 4.15B, the nullcline structure has not changed significantly; what has changed is the stability of the steady state. In Figure 4.15B, the steady state is a stable spiral point. In contrast, Figure 4.16B reveals an unstable spiral point in the center of the limit cycle. The close-up in Figure 4.17 shows how trajectories are repelled from the unstable steady state and converge toward the limit cycle from the inside.

In the following chapters we will see a variety of oscillatory phenomenon. Sustained limit cycle behaviours are generated from two necessary ingredients: negative feedback and nonlinearity. Many biological oscillators can be classified as either *delay oscillators* or *relaxation oscillators*. The periodic behaviour of delay oscillators is caused by a lag in a negative feedback loop, which causes repeated rounds of accumulated activity. Relaxation oscillators exhibit an interplay of positive and negative feedback. Positive feedback causes these system to display near-bistable behaviour; the negative feedback causes cyclic transfers between the two quasi-stable conditions. Relaxation oscillators exhibit behaviour at different timescales, with slow negative feedback operating over fast positive feedback. This results in sudden switches from one state to the other, leading to sharp "pulse-like" oscillations. Delay oscillators, in contrast, tend to exhibit smoothly varying time-courses.

Model (4.10) is best described as a relaxation oscillator. The allosteric activation introduces

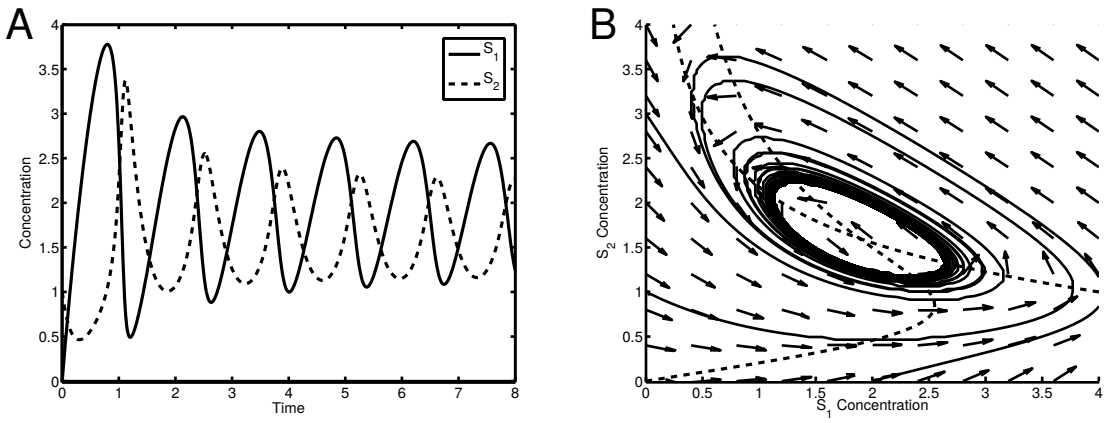

Figure 4.16: Model (4.10) with strong nonlinearity. **A.** This time series shows convergence to sustained periodic behaviour. **B.** In this phase portrait all trajectories converge to a cyclic track called a limit cycle. The steady state at the intersection of the nullclines is an unstable spiral point. Parameter values as in Figure 4.15 except $n = 2.5$.

both positive feedback (increasing the rate of S_2 production) and negative feedback (depleting the pool of S_1, and so eventually stifling S_2 production). As the degree of cooperativity n is increased, the pulse-like nature of the oscillations becomes more pronounced, with spike-like rise-and-crash behaviours followed by longer intervals in the depleted state.

It is usually difficult to infer the existence of limit cycle oscillations directly from model structure. In the special case of two-species models, a result called the Poincaré-Bendixson Theorem can be used. This theorem states that if all trajectories are bounded (i.e. do not escape by diverging to infinity), and the system exhibits no stable steady states, then there must be a limit cycle. The intuition is that the trajectories have to settle somewhere; since they cannot diverge, or settle to a steady state, the only remaining option is convergence to a limit cycle.

Exercise 4.3.1 The Brusselator is a theoretical model of an oscillatory chemical reaction network (developed at the Free University of Brussels). The network is

$$\begin{aligned} &\xrightarrow{k_1} && X \\ X &\xrightarrow{k_2} && Y \\ 2X + Y &\xrightarrow{k_3} && 3X \\ X &\xrightarrow{k_4} \end{aligned}$$

a) Verify that the model is

$$\frac{d}{dt}x(t) \quad = \quad k_1 - k_2 x(t) + k_3 x(t)^2 y(t) - k_4 x(t)$$

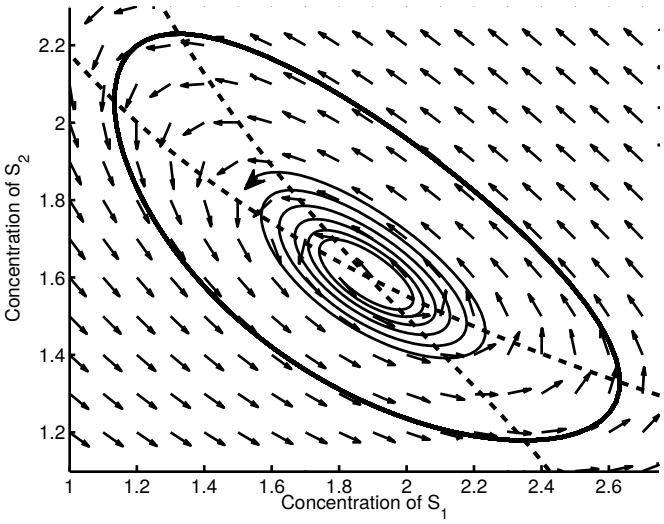

Figure 4.17: Model (4.10) with strong nonlinearity: unstable steady state. Trajectories that start near the unstable steady state spiral away from it, eventually converging to the limit cycle. Parameter values as in Figure 4.16.

$$\frac{d}{dt}y(t) \quad = \quad k_2 x(t) - k_3 x(t)^2 y(t).$$

b) Find the steady state of the system.
c) Take $k_2 = 2$ (time^{-1}), $k_3 = \frac{1}{2}$ (time^{-1} $\cdot$ concentration^{-1}) and $k_4 = 1$ (time^{-1}). Use linearized stability analysis to verify that the steady state is unstable when $0 < k_1 < \sqrt{2}$. It can be shown that trajectories do not diverge. The Poincare-Bendixson Theorem thus indicates that the system exhibits limit cycle oscillations for these k_1 values. □

In our discussions of bistability and limit cycle oscillations, we saw that a model's qualitative behaviour can change as parameters values vary. We will next introduce an analytic approach that provides a deeper insight into these changes in model behaviour.

4.4 Bifurcation Analysis

In most cases, the position of a model's steady state shifts if the model parameters are changed. For instance, Figure 4.18 shows the steady state concentration of S_1 in model (4.1) as the parameter k_1 varies. In an experimental context, this plot would be called a *dose-response curve*; when it is constructed from a model, it is called a *continuation diagram*.

As we have seen, variation in parameter values can cause qualitative changes in long-term system behavior, e.g. changes in the number of steady states or in their stability properties. Parameter values at which such changes occur are called *bifurcation points*; a continuation diagram on which bifurcation points appear is called a **bifurcation diagram**.

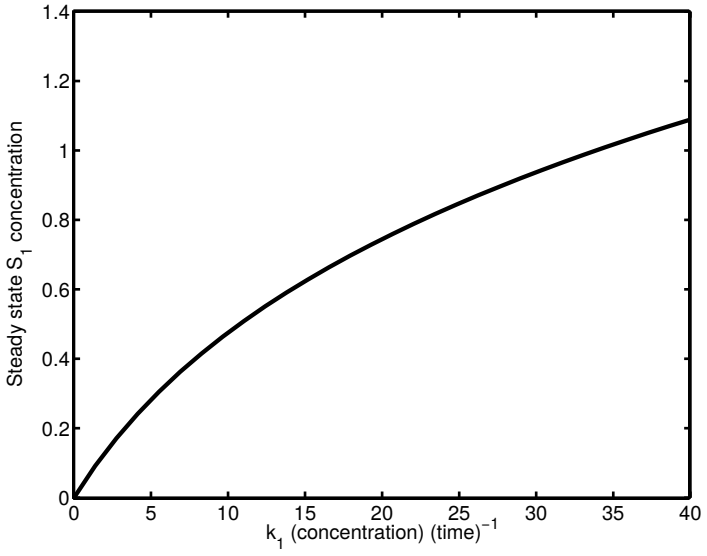

Figure 4.18: Continuation diagram. The steady state of species S_1, from model (4.1), is shown as a function of the value of parameter k_1. In an experimental context, this would be called a dose-response curve. Other parameter values as in Figure 4.2.

Exercise 4.4.1 Consider the differential equation

$$\frac{d}{dt}x(t) = (a-1)x(t).$$

By determining the sign of the rate of change $\frac{dx}{dt}$ for positive and negative values of x, verify that the steady state at $x = 0$ is stable if $a < 1$, and unstable if $a > 1$. The parameter value $a = 1$ is thus a bifurcation point for this system. □

Figure 4.19, shows a bifurcation diagram for the symmetric reaction network modelled by (4.2). The phase plots in Figure 4.19A show the nullclines at four different values of parameter k_1. As k_1 varies, the s_1-nullcline (gray curve) shifts, changing the number of points at which the nullclines intersect. The bifurcation diagram in Figure 4.19B shows the steady-state behaviour of $[S_1]$ as k_1 varies. The points corresponding to each subplot in Panel A are marked. This S-shaped bifurcation curve is characteristic of bistable systems. The points where the bifurcations occur (at $k_1 = 16.1$ and $k_1 = 29.0$) are called *saddle-node* bifurcations (because they occur when an unstable saddle point and a stable node come together). Between these bifurcation points, three steady states co-exist.

Figure 4.19B reflects the ability of this bistable system to act as a switch: an input that pushes parameter k_1 back and forth past the saddle-node bifurcations will toggle the system between low- and high-$[S_1]$ states. The intermediate bistable range introduces a lag into this switching action; over this interval, the state is not uniquely determined by the value of k_1, it also depends on the previous condition. The sketch in Figure 4.20A illustrates this behaviour. If the bistable range is entered from the high state, then the system remains in the high state over this interval. The

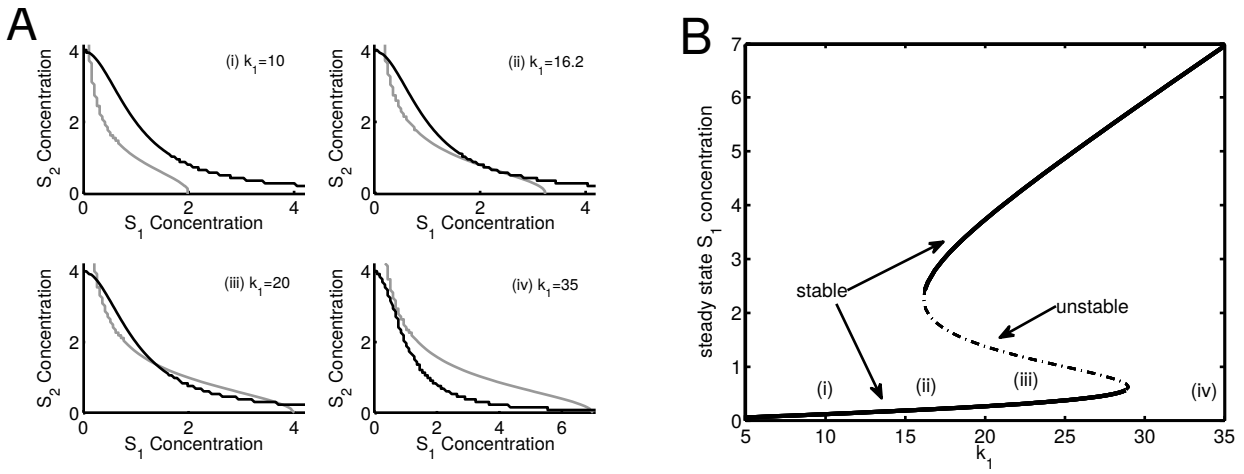

Figure 4.19: Bifurcation diagram for model (4.2). **A.** Nullclines at various values of k_1. As k_1 increases, the s_1-nullcline (gray curve) shifts: (i) at low k_1 there is a single steady state (low $[S_1]$, high $[S_2]$); (ii) at a higher value of k_1, a new steady state appears when a new intersection appears; (iii) at still higher values, three intersection points are exhibited—the system is bistable; (iv) finally, at high k_1 values, there is again a single intersection point (high $[S_1]$, low $[S_2]$). **B.** Bifurcation diagram showing the S_1 steady state concentration as a function of the value of parameter k_1. At low and high k_1 values, the system is monostable and exhibits a single stable steady state (solid curves). Over a mid-range interval, the two stable steady states co-exist, separated by an unstable steady state (dashed curve). The k_1 values at which steady states appear or disappear are saddle-node bifurcations. The k_1 values represented in Panel A are indicated. Parameter values: $k_2 = 20$ (concentration $\cdot$ time^{-1}), $K_1 = K_2 = 1$ (concentration), $k_3 = k_4 = 5$ (time^{-1}), $n_1 = n_2 = 2$. Units are arbitrary.

opposite holds if the bistable region is entered from the low state. This 'path-dependent' property is referred to as *hysteresis*. As the system cycles back and forth between the two states, it follows a *hysteresis loop*, in which transitions between the two states occur at two separate threshold values (i.e. at the two bifurcation points). Some switches are irreversible. As shown in Figure 4.20B, if one of the two saddle-node bifurcations is outside the range of relevant parameter values, then the system executes a one-way transition between the two states.

Next, we turn to the oscillatory model (4.10). Recall that for this model, oscillatory behaviour is dependent on the degree of cooperativity n. A bifurcation diagram for this system is shown in Figure 4.21. For small values of n, a single stable steady state is shown. At $n = 2.4$ a change occurs—the steady state becomes unstable, and a limit cycle appears. The bifurcation diagram shows both the change in stability and the upper and lower bounds of the limit cycle oscillations.

The bifurcation in Figure 4.21 occurs when the stability of the steady state changes. From our discussion of linearized stability analysis (Section 4.2.2), we know that this change occurs when eigenvalues of the Jacobian at the steady state transition from having negative real part (stable) to positive real part (unstable). This steady state in model (4.10) is a spiral point, and so the eigenvalues are complex numbers. The bifurcation in Figure 4.21, in which a pair of complex-valued eigenvalues transition between negative and positive real part, is called a *Hopf bifurcation*.

Bifurcation diagrams provide insight into the *robustness* of system behaviour. A behaviour is called robust if it is not significantly affected by disturbances. This is indicated by a bifurcation diagram: if a system is operating far from any bifurcation points, then perturbations are unlikely

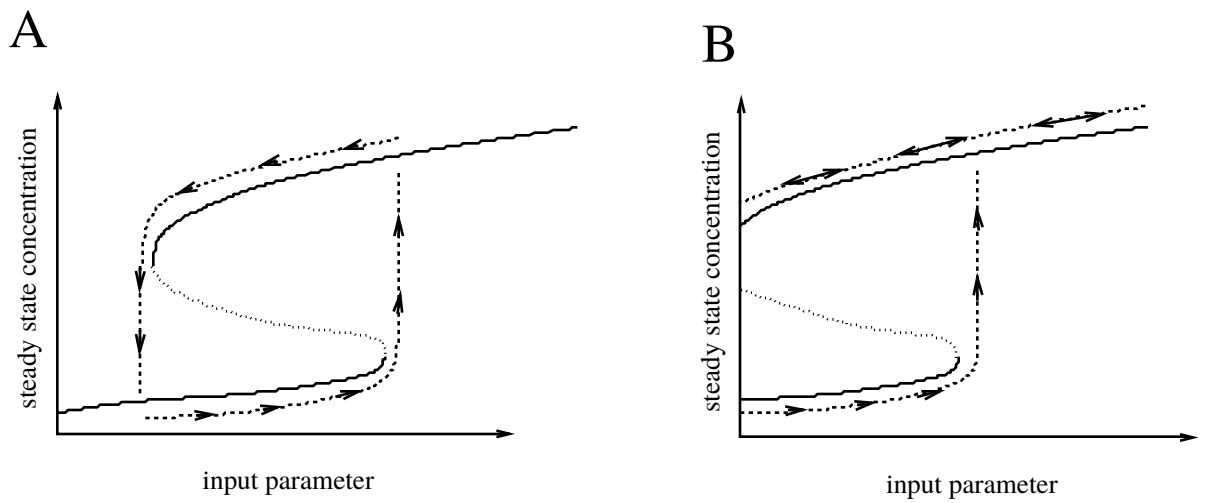

Figure 4.20: Switching in bistable systems. **A.** Hysteresis loop. Changes in the input parameter can push the system from one steady state to the other. Over the intermediate bistable region, the state depends on the recent past. Transitions between the two states occur abruptly at the bifurcation points. **B.** Irreversible switching. If one of the two bifurcation points is inaccessible, the system can become trapped in one of the steady states.

to result in a qualitative change in system behaviour; alternatively, the behaviour of a system operating near a bifurcation point may change dramatically in response to a disturbance. In the next section we will address another tool for analysing robustness: parametric sensitivity analysis.

4.5 Sensitivity Analysis

Continuation and bifurcation diagrams illustrate how model behaviour depends on parameter values. The general study of this dependence is called **(parametric) sensitivity analysis**. It can be divided into *global sensitivity analysis*—which addresses wide variations in parameter values—and *local sensitivity analysis*—which addresses small variations around a nominal operating condition.

Global sensitivity analysis typically involves sampling the space of parameter values and determining the corresponding system behaviour; statistical methods are usually employed to analyse the results.

In this section we will address local sensitivity analysis, which employs linearized model approximations. There is a long tradition using local sensitivity analysis to study biochemical networks (through Metabolic Control Analysis (MCA) and Biochemical Systems Theory (BST)).

4.5.1 Local sensitivity analysis

Consider the simple reaction scheme:

$$\longrightarrow S \longrightarrow$$

Suppose the rate of production is maintained at a constant rate V_0 while the rate of consumption is described by Michaelis-Menten kinetics as $\frac{V_{\max} s}{K_M + s}$, where $s = [S]$. The steady state concentration

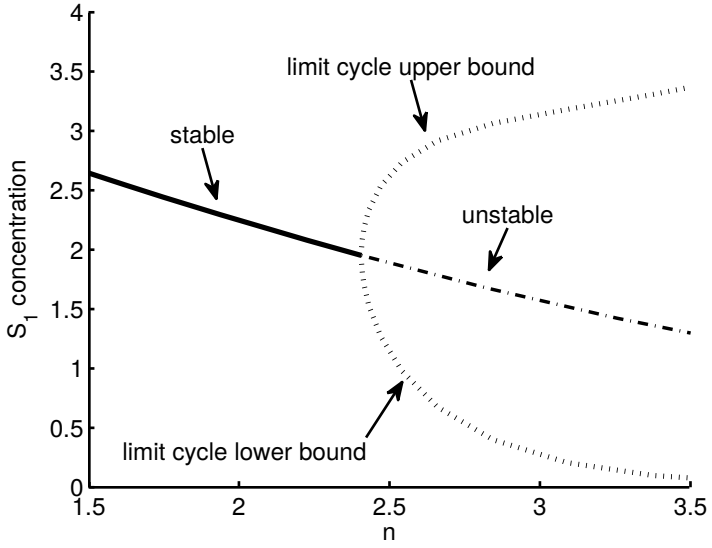

Figure 4.21: Bifurcation diagram for the autocatalytic model (4.10). For small n values, a single stable steady state is shown. At higher n values, this steady state is unstable. At the bifurcation point ($n = 2.4$) a stable limit cycle is born; the two dotted curves show the maximal and minimal concentrations reached by the limit cycle. The transition point is called a Hopf bifurcation. Parameter values as in Figure 4.15.

s^{ss} is characterized by

$$V_0 = \frac{V_{\max} s^{ss}}{K_M + s^{ss}}.$$

Solving for s^{ss}, we find

$$s^{ss} = \frac{V_0 K_M}{V_{\max} - V_0}. \tag{4.11}$$

Now, suppose that $V_{\max}$ is varied while V and K_M are held fixed. Equation (4.11) then defines the steady state concentration as a function of $V_{\max}$. For concreteness, we take $V_0 = 2$ mM/min and $K_M = 1.5$ mM. In that case, equation (4.11) becomes

$$s^{ss} = \frac{3}{V_{\max} - 2}. \tag{4.12}$$

This relationship is plotted in Figure 4.22 (a continuation diagram).

Because most models do not admit explicit steady-state formulas, construction of continuation curves generally requires significant computational effort. As an alternative, parametric sensitivities provide an easily calculated description of the continuation curve near a nominal parameter value.

The **absolute local sensitivity** of a steady state s^{ss} with respect to a variable p is defined as the rate of change of s^{ss} with respect to p, that is, as $\frac{ds^{ss}}{dp}$. This is the slope of the tangent to the continuation curve (Figure 4.22). This sensitivity coefficient can be used to predict the effect of small perturbations Δp at the parameter value $p = p_0$, through the linearization formula:

$$s^{ss}(p_0 + \Delta p) \approx s^{ss}(p_0) + \Delta p \, \frac{ds^{ss}}{dp}. \tag{4.13}$$

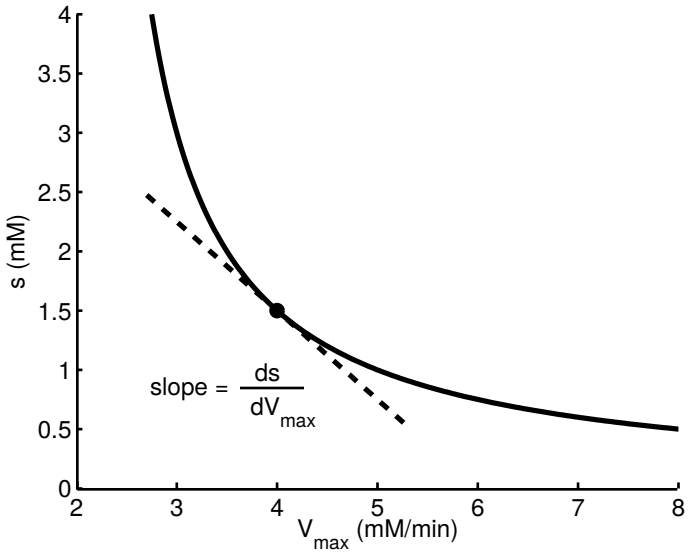

Figure 4.22: Local sensitivity. The solid continuation curve shows the steady state as a function of the parameter $V_{\max}$. The dashed line is the tangent at $V_{\max} = 4$ mM/min. The slope of this tangent is the absolute local sensitivity coefficient, which describes the effect of small changes in $V_{\max}$ on the steady state.

Returning to our example, from the explicit formula for steady state in equation (4.12), the absolute local sensitivity coefficient with respect to $V_{\max}$ can be calculated directly:

$$\frac{ds^{ss}}{dV_{\max}} = \frac{d}{dV_{\max}}\left(\frac{V_0 K_M}{V_{\max} - V_0}\right) = \frac{-3}{(V_{\max} - 2)^2}. \tag{4.14}$$

Choosing a nominal value of $V_{\max} = 4$ mM/min, we find a sensitivity coefficient of $\frac{ds^{ss}}{dV_{\max}} = -0.75$ min (Figure 4.22). Thus an increase of, say, 0.1 mM/min in $V_{\max}$ leads to a $0.75(0.1) = 0.075$ mM decrease in s^{ss}, for $V_{\max}$ near 4 mM/min (by applying equation (4.13) with $p_0 = 4$ mM/min and $\Delta p = 0.1$ mM/min).

Although this sensitivity coefficient can be used to make predictions, it is not usually employed directly. An improved sensitivity measure describes the *relative* effect of perturbations. We define the **relative sensitivity** as

$$\frac{ds^{ss}/s^{ss}}{dp/p} = \frac{p}{s^{ss}}\frac{ds^{ss}}{dp}.$$

The relative sensitivity relates the size of a relative perturbation in p to a relative change in s^{ss}. Referring back to equation (4.12), we find that at $V_{\max} = 4$ mM/min, the relative sensitivity coefficient of s^{ss} with respect to $V_{\max}$ is $\frac{V_{\max}}{s^{ss}}\frac{ds^{ss}}{dV_{\max}} = (\frac{4}{1.5})(-0.75) = -2$. Thus a 1% increase in $V_{\max}$ results in a 2% decrease in s^{ss}.

Relative sensitivity coefficients are frequently used to provide a concise description of model behaviour. These coefficients provide insight into robustness: if the system shows a small sensitivity coefficient with respect to a parameter, then behaviour is robust with respect to perturbations of

that parameter. In contrast, large sensitivity coefficients (positive or negative) suggest 'control points' at which interventions will have significant effects.

Exercise 4.5.1 Starting from equation (4.11), verify that the relative sensitivity coefficients of s^{ss} with respect to K_M is equal to one, regardless of the parameter values. □

4.5.2 Determining local sensitivity coefficients

Numerical approximation

Local sensitivity coefficients are typically determined by simulation. The sensitivity coefficient at a parameter value $p = p_0$ can be determined by simulating the model at $p = p_0$ and at another nearby value $p = p_0 + \Delta p_0$, where Δp_0 should normally be chosen less than a 5% deviation from p_0. The derivative $\frac{ds^{ss}}{dp}$ at $p = p_0$ can then be approximated by

$$\frac{ds^{ss}}{dp} \approx \frac{s^{ss}(p_0 + \Delta p_0) - s^{ss}(p_1)}{\Delta p_0}. \tag{4.15}$$

This ratio can then be scaled by p_0/s^{ss} to arrive at the relative sensitivity. When using this approximation, care must be taken to avoid the significant round-off errors that can occur when calculating the ratio of two small numbers. (To ensure accuracy, the approximation can be calculated for a handful of Δp_0 values, e.g. at 1%, 3% and 5% displacements from p_0. If these approximations do not agree, then a more accurate simulation procedure may be needed.)

Exercise 4.5.2 Verify the accuracy of the finite difference approach by using equation (4.15) to approximate the absolute sensitivity coefficient in equation (4.14) (at the nominal value of $V_{\max} = 4$ mM/min). Calculate approximations with $\Delta p_0 = 0.2$ (5% deviation) and $\Delta p_0 = 0.04$ (1% deviation). □

Implicit differentiation

When an explicit formula for steady state is available (as in equation (4.12)), sensitivity coefficients can be determined by direct differentiation. For most models, no such steady-state formula is available. Nevertheless, sensitivity coefficients can be derived by implicit differentiation of the differential equation model, as in the following exercise.

Exercise 4.5.3 Consider a species S that is consumed at rate $k_2[S]$ and inhibits its own production, so that it is produced at rate $k_1/(1 + [S]^n)$. The steady state concentration s is then given by

$$0 = k_1/(1 + s^n) - k_2 s.$$

Use implicit differentiation (reviewed in Appendix B) to determine the absolute sensitivity coefficient $\frac{ds}{dk_1}$ and verify that it is positive for all values of k_1, k_2, and n. □

4.6 *Parameter Fitting

Chapters 2 and 3 addressed techniques for model construction, but gave no indication of how the values of model parameters should be chosen. The task of finding appropriate parameter values is called *model calibration* or *parameter fitting*.

Some parameters can be measured directly. For instance, rates of degradation can be determined from observations of half-lives, and specialized enzymological assays have been developed to determine the kinetic parameters of enzyme catalysis. However, in constructing models for systems biology, most model parameters are not measured directly. Instead, parameter values are assigned by fitting model behaviour to corresponding observations of system behavior. We will next outline the most commonly used parameter calibration approach, called *least-squares fitting*.

Suppose observations have been made of a biological system, and a model structure (i.e. a network with reaction kinetics) has been chosen. To be concrete, suppose that the model involves three species concentrations s_1, s_2, s_3, and depends on two parameters p_1 and p_2:

$$\begin{aligned}\frac{d}{dt}s_1(t) &= f_1(s_1(t), s_2(t), s_3(t), p_1, p_2)\\ \frac{d}{dt}s_2(t) &= f_2(s_1(t), s_2(t), s_3(t), p_1, p_2)\\ \frac{d}{dt}s_3(t) &= f_3(s_1(t), s_2(t), s_3(t), p_1, p_2).\end{aligned}$$

Depending on the experimental observations that have been made, corresponding simulations of the model can be carried out. For instance, observations of the steady-state concentrations correspond directly to the model's steady state: s_1^{ss}, s_2^{ss}, s_3^{ss}. Time-course data can be mimicked by sampling multiple time-points along a model trajectory. In most cases, it is not possible to measure all of the individual reactant species.

The goal of parameter fitting is to determine the parameter values for which model simulation best matches experimental data. The accuracy of the model can be assessed by comparing the model predictions to each of the experimental observations. This collection of comparisons can be combined into a single measure of the quality of fit. For the model described above, if steady-state observations of the concentrations are available (denoted s_i^{obs}) the *sum of squared errors* is defined by

$$\text{SSE}(p_1, p_2) = \left(s_1^{ss}(p_1, p_2) - s_1^{obs}\right)^2 + \left(s_2^{ss}(p_1, p_2) - s_2^{obs}\right)^2 + \left(s_3^{ss}(p_1, p_2) - s_3^{obs}\right)^2.$$

(The errors are squared to avoid cancellation between terms of opposite sign. A relative SSE can also be used, in which the error terms are scaled by the observations.)

When replicate observations are available, the predictions are usually compared to the mean of the replicates. The error terms can then be inversely weighted by the variance in the replicates, so that observations with high variability (in which we have less confidence) make a reduced contribution to the total error.

The *least-squares fit* correspond to the parameter values that minimize the sum of squared errors. This parameter set can be found by numerical function-minimization techniques. Although fitting to data almost always demands numerical calculations, we can illustrate the general principles with a simple example, as follows. Consider the reaction chain

$$\xrightarrow{k_1} S_1 \xrightarrow{k_2} S_2 \xrightarrow{k_3} \tag{4.16}$$

where the parameters k_1, k_2, and k_3 are mass-action rate constants. The reaction rates are then k_1, $k_2[S_1]$ and $k_3[S_2]$. We will illustrate least-squares fitting of the model parameters in three separate scenarios.

Case I. Suppose the consumption rate of S_2 has been measured directly: $k_3 = 4$ mM/min, and that steady state measurements have been made: $s_1^{obs} = 5$ mM, $s_2^{obs} = 2$ mM. In this case, an exact model fit can be found. We begin by solving for the model steady-state concentrations:

$$s_1^{ss} = \frac{k_1}{k_2} \qquad s_2^{ss} = \frac{k_2 s_1^{ss}}{k_3} = \frac{k_1}{k_3}.$$

The sum of squared errors is then

$$\begin{aligned} \text{SSE} &= \left(s_1^{ss}(k_1,k_2,k_3) - s_1^{obs}\right)^2 + \left(s_2^{ss}(k_1,k_2,k_3) - s_2^{obs}\right)^2 \\ &= \left(\frac{k_1}{k_2} - 5\right)^2 + \left(\frac{k_1}{k_3} - 2\right)^2 \end{aligned}$$

This error takes its minimum value (of zero) when

$$\frac{k_1}{k_2} = 5 \text{ mM} \qquad \text{and} \qquad \frac{k_1}{k_3} = 2 \text{ mM}. \tag{4.17}$$

Because we know $k_3 = 4$ mM/min, we can solve for $k_1 = 8$/min and $k_2 = \frac{8}{5}$/min.

Case II. Suppose now that the same steady state measurements have been made ($s_1^{obs} = 5$ mM, $s_2^{obs} = 2$ mM), but k_3 is unknown. In this case we have the same error function:

$$\text{SSE} = \left(\frac{k_1}{k_2} - 5\right)^2 + \left(\frac{k_1}{k_3} - 2\right)^2,$$

but we cannot determine a unique parameter set that minimizes this function. Solving equations (4.17) indicates that the error will be zero whenever

$$k_2 = \frac{k_1}{5} \qquad \text{and} \qquad k_3 = \frac{k_1}{2},$$

regardless of the value of k_1. In this case, the fitting problem is called *underdetermined*, since there are multiple equivalently good solutions. Unfortunately, parameter calibration of system biology models is often underdetermined, because it is a challenge to collect the experimental data needed to fit dynamic models. In such cases, model reduction techniques can sometimes be employed to reduced the number of parameters in the model.

Case III. Suppose that the value $k_3 = 4$ mM/min is known, and that steady state observations have been made in two conditions: in the control condition, $s_1^{obs} = 5$ mM, $s_2^{obs} = 2$ mM, while in the experimental condition, the (unknown) production rate k_1 has been reduced by 90% and measurements have been made of $s_1^{obs} = 0.5$ mM, $s_2^{obs} = 0.3$ mM.

In this case there are four terms in the sum of squared errors. The steady states in the experimental condition are

$$s_2^{ss} = \frac{k_1/10}{k_2} \qquad s_2^{ss} = \frac{k_1/10}{k_3},$$

so we have

$$\text{SSE} = \left(\frac{k_1}{k_2} - 5\right)^2 + \left(\frac{k_1}{4} - 2\right)^2 + \left(\frac{k_1/10}{k_2} - 0.5\right)^2 + \left(\frac{k_1/10}{4} - 0.3\right)^2.$$

There are *no* choices of k_1 and k_2 that will make this error equal to zero; this fitting problem is *overdetermined*. Overdetermined fits are caused by inaccuracies in model formulation and errors in experimental measurements. The 'solution' to an overdetermined fitting problem is a compromise parameter set that minimizes the resulting error.

Exercise 4.6.1 Consider again the network (4.16). Suppose that the degradation rate $k_3 = 4$ mM/min has been measured directly, and that observations are made in two conditions, but only the pooled concentration of S_1 and S_2 can be measured. Consider two cases:
(i) Suppose that in the control condition $s_1^{obs} + s_2^{obs} = 6$ mM, while in the experimental condition, the production rate k_1 has been reduced by 90% and the resulting observation is $s_1^{obs} + s_2^{obs} = 0.6$ mM. Perform a least-squares fit.
(ii) Suppose that in the control condition $s_1^{obs} + s_2^{obs} = 6$ mM, while in the experimental condition, the rate constant k_2 has been reduced by 90% and the resulting observation is $s_1^{obs} + s_2^{obs} = 18$ mM. Perform a least-squares fit.
How does your analysis in cases (i) and (ii) compare? Explain the difference.

□

4.7 Suggestions for Further Reading

- **Nonlinear Dynamics:** An accessible introduction to bistability, oscillations, and bifurcations can be found in the book *Nonlinear Dynamics and Chaos* (Strogatz, 2001). More formal treatments of nonlinear dynamics appear in many texts on differential equations, including *Elementary Differential Equations and Boundary Value Problems* (Boyce and DiPrima, 2008).

- **Sensitivity Analysis:** Techniques for global sensitivity analysis are introduced in *Global Sensitivity Analysis: The Primer* (Saltelli *et al.*, 2008). Local sensitivity analysis for chemical systems is addressed in *Parametric Sensitivity in Chemical Systems* (Varma *et al.*, 2005). Several applications of local sensitivity analysis to systems biology are reviewed in (Ingalls, 2008).

- **Parameter Fitting:** An introduction to parameter fitting in systems biology, including coverage of a range of computational function-minimization techniques, can be found in *Systems Biology: a textbook* (Klipp *et al.*, 2009).

4.8 Problem Set

4.8.1 Phase-line analysis. Phase analysis can be applied to systems of a single dimension. The phase portrait of a one-dimensional system lies on a *phase line*. For example, the phase portrait of the system

$$\frac{dx(t)}{dt} = x^2(t) - x(t) = x(t)(x(t) - 1),$$

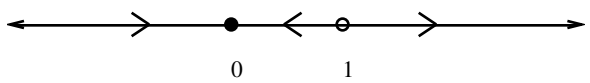

Figure 4.23: Phase line for Problem 4.8.1.

is shown in Figure 4.23, with the open circle indicating an unstable steady state, the closed circle indicating a stable steady state, and the arrows indicating the direction of motion.
a) Sketch the phase lines of the following one-dimensional systems.

$$\begin{aligned}
\text{i)} \quad \frac{d}{dt}V(t) &= V^3(t) - V(t) \\
\text{ii)} \quad \frac{d}{dt}r(t) &= r^4(t) - 3r^2(t) + 2 \\
\text{iii)} \quad \frac{d}{dt}w(t) &= \sin(w(t)) \\
\text{iv)} \quad \frac{d}{dt}p(t) &= p^3(t) - 2p^2(t) + p(t).
\end{aligned}$$

(Note, case (iv) involves a 'semi-stable' steady state.)
b) Use a phase line argument to confirm that a one-dimensional system can never display oscillatory behaviour.
c) Consider the simple model

$$\frac{d}{dt}s(t) = k - \frac{V_{\max}s}{K_M + s}$$

in which species s is produced at a fixed rate and consumed via Michaelis-Menten kinetics. Sketch a phase line for this system. Verify that the steady state is stable for any non-negative parameter values, provided $V_{\max} > k$.

4.8.2 Linear system: complex eigenvalues. Consider the system

$$\begin{aligned}
\frac{d}{dt}x_1(t) &= -x_1(t) + x_2(t) \\
\frac{d}{dt}x_1(t) &= -x_1(t) - x_2(t)
\end{aligned}$$

Find the eigenvalues of the Jacobian matrix. Determine the solution $(x_1(t), x_2(t))$ satisfying initial condition $(x_1(0), x_2(0)) = (1, 1)$ by substituting the general form of the solution (4.6) into the system of equations and solving for the parameters c_{ij}.

4.8.3 Linear system: dynamics. Consider the general linear system

$$\begin{aligned}
\frac{d}{dt}x(t) &= ax(t) + by(t) \\
\frac{d}{dt}y(t) &= cx(t) + dy(t).
\end{aligned}$$

Note that the steady state is $(x, y) = (0, 0)$. Choose 6 sets of parameter values (a, b, c, d) that yield the following behaviours

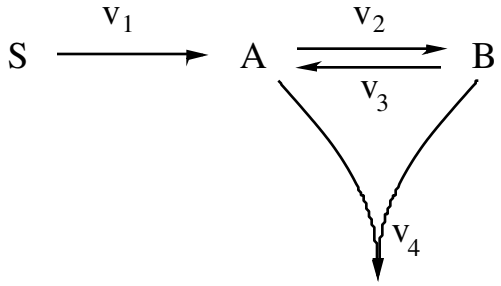

Figure 4.24: Reaction network for Problem 4.8.5.

i) stable node (real negative eigenvalues)
ii) stable spiral point (complex eigenvalues with negative real part)
iii) center (purely imaginary eigenvalues)
iv) unstable spiral point (complex eigenvalues with positive real part)
v) unstable node (real positive eigenvalues)
vi) saddle point (real eigenvalues of different sign)
In each case, prepare a phase portrait of the system, including the x and y nullclines, a direction field, and a few representative trajectories. Hint: recall from Exercise 4.2.4 that if either of the off-diagonal entries in the Jacobian matrix are zero, then the eigenvalues are simply the entries on the diagonal.

4.8.4 Phase portrait. Consider the nonlinear system

$$\begin{aligned} \frac{dx}{dt} &= \mu x - x^3 \\ \frac{dy}{dt} &= -y \end{aligned}$$

a) Take $\mu = -1$. Show that the system has a single steady state and characterize its stability by finding the eigenvalues of the Jacobian matrix at this point. Confirm your results by producing a phase portrait.
b) Repeat with $\mu = 1$. In this case there are three steady states.

4.8.5 Linearized Stability Analysis. Consider the chemical reaction network in Figure 4.24, with reaction rates v_i as labelled. Suppose the concentration of S is fixed at 1 mM, and that the reaction rates are given by mass action as: $v_1 = k_1[S]$, $v_2 = k_2[A]$, $v_3 = k_3[B]$ and $v_4 = k_4[A][B]$.
a) Write a pair of differential equations that describe the concentrations of A and B.
b) Presuming that $k_1 = 1/\text{min}$, $k_2 = 2/\text{min}$, $k_3 = 0.5/\text{min}$ and $k_4 = 1/\text{mM/min}$, determine the steady-state concentrations of A and B.
c) Evaluate the system Jacobian at the steady state found in (b) and verify that this steady state is stable.

4.8.6 Global dynamics from local stability analysis.
a) Consider the chemical reaction network with mass-action kinetics:

$$A + X \xrightarrow{k_1} 2X$$

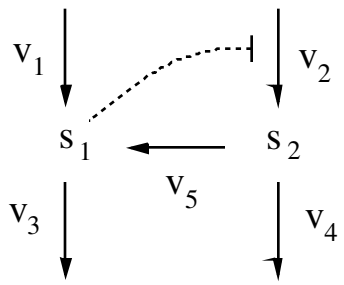

Figure 4.25: Reaction network for Problem 4.8.7.

$$X + X \xrightarrow{k_2} Y$$

$$Y \xrightarrow{k_3} B.$$

Assume that $[A]$ and $[B]$ are held constant.
i) Write a differential equation model describing the concentrations of X and Y.
ii) Verify that the system has two steady states.
iii) Determine the system Jacobian at the steady states and characterize the local behavior of the system near these points.
iv) By referring to the network, provide an intuitive description of the system behaviour starting from any initial condition for which $[X] = 0$.
v) Sketch a phase portrait for the system this is consistent with your conclusions from (iii) and (iv).
b) Repeat for the system

$$A + X \xrightarrow{k_1} 2X$$

$$X + Y \xrightarrow{k_2} 2Y$$

$$Y \xrightarrow{k_3} B.$$

In this case, you'll find that the non-zero steady-state is a center: it is surrounded by trajectories that are concentric circles.

4.8.7 Nullcline analysis. Consider the network in Figure 4.25. Suppose the reaction rates are given by

$$v_1 = V \qquad v_2 = f(s_1) \qquad v_3 = k_3 s_1$$
$$v_4 = k_4 s_2 \qquad v_5 = k_5 s_2$$

Suppose that the parameters V, k_3, k_4, and k_5 are positive constants, and that $f(s_1)$ takes positive values and is a *decreasing* function of s_1 (i.e. as the values of s_1 increase, the values of $f(s_1)$ decrease). By sketching the nullclines, demonstrate that this system cannot exhibit bistability.

4.8.8 Linearization. Consider the simple reaction system $\rightarrow S \rightarrow$, where the reaction rates are

$$\text{production: } V_0 \qquad\qquad \text{consumption: } \frac{V_{\max}[S]}{K_M + [S]}.$$

a) Write the differential equation that describes the dynamics in $[S]$. Find the steady state. Next, approximate the original system by linearizing the dynamics around the steady state. This approximation takes the form of a linear differential equation in the new variable $x(t) = s(t) - s^{ss}$.
b) Take parameter values $V_0 = 2$, $V_{\max} = 3$, and $K_M = 1$ and run simulations of the nonlinear and linearized systems starting at initial conditions $[S] = 2.1$, $[S] = 3$, and $[S] = 12$. Comment on the discrepancy between the linear approximation and the original nonlinear model.

4.8.9 Saddle-Node bifurcation. Consider the system

$$\frac{d}{dt}x(t) = \mu - x^2(t).$$

Draw phase lines (as in Problem 4.8.1) for $\mu = -1$, 0, 1. For this system, $\mu = 0$ is a bifurcation value. Use your one-dimensional phase portraits to sketch a bifurcation diagram for the system showing steady states of x against μ. Be sure to indicate the stability of each branch of steady states.

4.8.10 Pitchfork bifurcation. Recall from Problem 4.8.4 that the nonlinear system

$$\frac{dx}{dt} = \mu x - x^3 \qquad\qquad \frac{dy}{dt} = -y$$

exhibits different steady-state profiles depending on the value of the parameter μ. Sketch a bifurcation diagram showing steady states of x against μ. Your diagram should make it clear why the point $\mu = 0$ is referred to as a pitchfork bifurcation.

4.8.11 Bifurcation diagram: bistability. Consider model (4.2) with parameter values: $k_1 = k_2 = 20$ (concentration $\cdot$ time^{-1}), $K_1 = K_2 = 1$ (concentration), $k_3 = k_4 = 5$ (time^{-1}), and $n_2 = 2$. Use a software package to generate a bifurcation diagram showing the steady-state concentration of S_1 as a function of the parameter n_1. The system is bistable when $n_1 = 2$. Does the system become monostable at high n_1, at low n_1, or both?

4.8.12 Bifurcation diagram: limit-cycle oscillations. Consider the autocatalytic model (4.10), with parameter values $k_0 = 8$, $k_1 = 1$, $K = 1$, and $n = 2.5$. Use a software package to generate a bifurcation diagram showing the steady-state concentration of S_1 as a function of the parameter k_2. The system exhibits limit-cycle oscillations when $k_2 = 5$. Are the oscillations lost at high k_2, low k_2, or both?

4.8.13 Sensitivity analysis: reversible reaction. Consider the reversible reaction

$$A \underset{k_2}{\overset{k_1}{\rightleftharpoons}} A^*$$

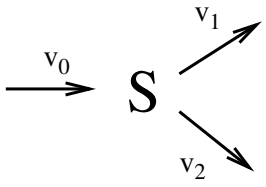

Figure 4.26: Reaction network for Problem 4.8.14.

with mass-action rate constants as shown. Let T be the total concentration of A and A^*.
a) Solve for the steady-state concentration of A^* and verify that an increase in k_1 leads to an increase in $[A^*]^{ss}$.
b) Use parametric sensitivity analysis to determine whether the steady state concentration of A^* is more sensitive to a 1% increase in T or a 1% increase in k_1. Does the answer depend on the values of the parameters?

4.8.14 Sensitivity analysis: branched network. Consider the branched network in Figure 4.26. Suppose the reaction rates are:

$$v_0 = V, \quad v_1 = k_1[S], \quad v_2 = k_2[S],$$

with V, k_1 and k_2 constant. Suppose that $k_1 > k_2$. Use sensitivity analysis to determine whether the steady state of $[S]$ is more sensitive to a 1% increase in k_1 or a 1% increase in k_2.

4.8.15 *Sensitivity coefficients in S-system models. The relative sensitivity coefficients defined in Section 4.5 can be formulated as ratios of changes in the logarithms of concentrations and parameter values:

$$\frac{p}{s^{ss}}\frac{ds^{ss}}{dp} = \frac{d\log(s^{ss})}{d\log(p)}.$$

For this reason, sensitivity coefficients are sometimes called *logarithmic gains*. Because S-system models (Section 3.5) involve linear relationships among logarithmic quantities, relative sensitivities reveal themselves immediately in these model.

Refer to the S-system model (3.22-3.23). Verify that relative sensitivities with respect to the rate constants α_i appear as coefficients in equations (3.24).

4.8.16 *Model fitting: time-series data. Consider the network

$$\xrightarrow{k_1} S \xrightarrow{k_2} \tag{4.18}$$

Suppose that the following time-series data is available for model fitting (in mM): $s(0) = 0$, $s(1) = 1$, $s(2) = 1.5$. Determine the corresponding model parameters. (The data can be fit exactly.) Recall from equation (2.6) the predicted time-course takes the form

$$s(t) = \left(s(0) - \frac{k_1}{k_2}\right) e^{-k_2 t} + \frac{k_1}{k_2}.$$

Hint: You will need to solve an equation of the form $ae^{-2k_2} + be^{-k_2} + c = 0$. This is a quadratic equation in $x = e^{-k_2}$.